

American University in Cairo

AUC Knowledge Fountain

Theses and Dissertations

Student Research

Fall 9-13-2020

Role of Ataxia Telangiectasia mutated in the repair of Magnetite Nanoparticles induced double strand breaks associated with Heterochromatin

Mie Mohamed Mounir

The American University in Cairo

Follow this and additional works at: <https://fount.aucegypt.edu/etds>

Recommended Citation

APA Citation

Mounir, M. (2020). *Role of Ataxia Telangiectasia mutated in the repair of Magnetite Nanoparticles induced double strand breaks associated with Heterochromatin* [Master's Thesis, the American University in Cairo]. AUC Knowledge Fountain.

<https://fount.aucegypt.edu/etds/1486>

MLA Citation

Mounir, Mie Mohamed. *Role of Ataxia Telangiectasia mutated in the repair of Magnetite Nanoparticles induced double strand breaks associated with Heterochromatin*. 2020. American University in Cairo, Master's Thesis. *AUC Knowledge Fountain*.

<https://fount.aucegypt.edu/etds/1486>

This Master's Thesis is brought to you for free and open access by the Student Research at AUC Knowledge Fountain. It has been accepted for inclusion in Theses and Dissertations by an authorized administrator of AUC Knowledge Fountain. For more information, please contact thesisadmin@aucegypt.edu.

**Role of Ataxia Telangiectasia Mutated in the Repair of Magnetite
Nanoparticles Induced Double Strand Breaks Associated with
Heterochromatin**

Mie Mohamed Mounir

B.Sc. in Pharmaceutical Sciences

**under supervision of Dr. Andreas Kakarougkas, PhD
Assistant Professor of Cell and Molecular Biology**

**Submitted in partial fulfilment of the requirements for the degree of
Master of Science in Biotechnology**

School of Sciences and Engineering

The American University in Cairo

2020

Keywords

Magnetite Nanoparticles, Particulate Matter, Ataxia telangiectasia mutated, Double Strand Breaks, DNA repair, Heterochromatin.

Abstract

Magnetite nanoparticles particulate matter pollution is escalating in large cities like New Mexico, Manchester city, Cairo, and New Delhi. Combustion derived Magnetite nanoparticles was found deposited in internal vital organs of deceased residents of urban areas. A great deal of research focused on the genotoxic and cytotoxic effects of Magnetite Nanoparticles (MNPs). In our work we focus on the mechanisms employed in DNA repair of higher chromatin structures. We employed the sensitive analysis of anti γ -H2AX to detect and monitor the repair of DSBs following exposure to MNPs. A 2- fold delay in the repair of heterochromatin associated DSBs in comparison with euchromatin was detected. The slow repairing heterochromatin γ -H2AX foci were found almost exclusively at the peripheries of the chromocenters, marking the physical barrier that the compacted chromatin impose on the extension of the DNA repair signal. The heterochromatin associated DSBs constituted 10.3% of the original DSBs initially introduced, similarly the fraction of DSBs that requires ATM for DNA repair constitutes about 10-25%. No visible structural changes happened in heterochromatin chromocentres during the repair. On Inhibition of ATM a repair defect in the heterochromatin DSBs was evident post exposure to MNPs, comparable to the repair defect imparted after exposure to Neocarzinostatin (NCS). This repair defect could not be compensated by other PIKKs (ATR and DNA PKcs). Therefore, ATM is essential for the transient relaxation of the nucleosome to allow the extension of the DNA repair machinery. Individuals lacking a functional ATM protein, will lack the ATM dependent chromatin relaxation and extension of repair machinery. So, they would be prone to accumulate mutations in the repetitive satellite pericentromeres, centromeres and telomeres, imparting a MNPs sensitivity to those individuals.

Table of Contents

Keywords	2
Abstract	3
Table of Contents	4
Table of Figures	7
List of Abbreviations	9
Original Authorship Statement	11
Acknowledgments	12
1. Introduction	14
2. Literature Review	16
2.1 Magnetite nanoparticles as an industrial biological hazard.	16
2.2. Role of reactive oxygen species in Magnetite Nanoparticles genotoxicity	18
2.3 Ataxia Telangiectasia disorder, DNA double strand breaks and DNA repair.	19
2.4. Role of Ataxia Telangiectasia Mutated in DNA double strand breaks repair.....	21
2.5 Ataxia Telangiectasia Mutated activation by oxidative stress.	24
2.6 Factors controlling heterochromatinization.	25
2.7 Ataxia Telangiectasia Mutated and chromatin modulation post ionizing radiation.....	29
3. Aim of Work	32
3.1 Monitoring the repair kinetics of DNA double strand breaks associated with heterochromatin and euchromatin post exposure to Magnetite nanoparticles.	32

3.2 Revealing of the mechanism required for the repair of heterochromatin associated DNA double strand breaks post Magnetite nanoparticles exposure.	32
3.3 Evaluation and comparison of the repair mechanisms required for the repair of heterochromatin associated DNA double strand breaks post Magnetite nanoparticles and Neocarzinostatin exposure.	33
4. Materials and Methods	34
4.1 Cell line	34
4.2 Chemicals and nanoparticles.....	35
4.3 Nanoparticles Dispersion.	35
4.4 Cell Culturing.....	35
4.5 Immunostaining technique.....	35
4.6 Dose response of Magnetite nanoparticles in L929 cell line.	36
4.7 Assessment of DNA damage repair associated with heterochromatin after exposure to MNP.	36
4.8 Assessment of DNA damage repair associated with heterochromatin after exposure to Neocarzinostatin and inhibition of Ataxia telangiectasia mutated.....	43
4.9 Assessment of DNA damage repair associated with heterochromatin after exposure to MNP and inhibition of ATM.....	44
4.10 Alkaline comet assay (Single cell gel electrophoresis).....	45
4.11 Statistical Analysis.....	47
5. Results	48

5.1 Magnetite nanoparticles DNA double strand breaks dose response in L929.	48
5.2 Alkaline comet assay Single cell gel electrophoresis	50
5.3 Heterochromatin Vs euchromatin repair kinetics after exposure to Magnetite nanoparticles.	
51	
5.4 Ataxia telangiectasia Mutated inhibition and Heterochromatin repair post Magnetite Nanoparticles.....	56
6. Discussion.....	60
7. Conclusion.....	65
8. Prospects.....	66
9. References.....	67

Table of Figures

Figure 1 Transmission electron micrograph of thin brain sections.....	17
Figure 2 ATM response to DNA double strand breaks.	21
Figure 3 Structural model for ATM.....	22
Figure 4 Diagram showing heterochromatinization pathway.	28
Figure 5 Schematic diagram for KAP-1 domains.....	30
Figure 6 Localization of heterochromatic markers H3K9me3, CENP-A, KAP-1, and HP1.....	34
Figure 7 L929 nucleus stained with DAPI, showing densely stained regions of heterochromatin.	38
Figure 8 Screen shots showing the use of color composite tool on Imageview software to collate all DAPI images into one.....	39
Figure 9 L929 nucleus stained with anti- γ H2AX (Ser139) (Merck Millipore, 05-636), anti-mouse secondary antibody Alexafluor488 (Thermofisher scientific, A21200).	40
Figure 10 Screen shot showing the use of color composite tool on Imageview software to collate all γ -H2AX foci images into one.	41
Figure 11 Merged images of L929 nucleus.	42
Figure 12 Screen shot showing the use of color composite tool on Imageview software to overlay the collated γ -H2AX foci image and the collated DAPI into one.....	42
Figure 13 Counting of γ -H2AX foci from overlaid images of L929.....	43
Figure 14 Image analysis on Cometscore software.	46
Figure 15 γ - H2AX foci in L929 cell line after exposure to increasing concentrations to MNPs.49	
Figure 16 Percentage of DNA in comet tails in L929 cell line post exposure to MNPs.	50
Figure 17 γ -H2AX foci resolution at 24 hours post MNP.....	52

Figure 18 Persisting clumps of MNP around nuclei of L929. 53

Figure 19 Heterochromatin and Euchromatin repair kinetics in L929 cell line. 54

Figure 20 γ -H2AX foci localizing around high intensity DAPI stained regions of heterochromatin. 56

Figure 21 Initial γ -H2AX foci formed at 2 hours in MNP treated vs MNP/ATMi treated L929 cells. 57

Figure 22 Heterochromatin vs euchromatin repair kinetics post MNP in L929 ATM inhibited cells. 59

List of Abbreviations

A-T	Ataxia telangiectasia disorder
ATM	Ataxia Telangiectasia Mutated
ATMi	ATM inhibitor
ATR	ATM- and Rad3- related
CDNP	Combustion-derived nanoparticles
DAPI	4',6-diamidino-2-phenylindole
DNA-PKcs	DNA protein kinase catalytic subunit
DSB	Double strand break
EU	Euchromatin
FAT	FRAP-ATM-TRRAP
HC	Heterochromatin
HDAC	Histone deacetylase
HEAT	Huntingtin, elongation factor 3, a subset of protein phosphatase 2A, TOR1
HP1	H3-trimethyl K9 binding protein
IR	Ionizing Radiation
KAP-1	Krüppel associated box (KRAB) associated protein-1
LMA	Low melting point agarose

MNPs	Magnetite Nanoparticles
Mre11	Meiotic recombination 11
MRN	Mre11, Rad50 and NBN
NCS	Neocarzinostatin
PI3K	Phosphoinositide 3 Kinase
PIKK	Phosphoinositide 3-kinase (PI3K)- related kinase
pKap-1	Phosphorylated Kap-1 at S824
ROS	Reactive Oxygen Species
8-OH-dg	8-hydroxy-2' -deoxyguanosine

Original Authorship Statement

Our work was not previously submitted to fulfill requirements of any degree or award at the American University in Cairo or any other research institution. I confirm that to the best of my knowledge no materials published by other authors mentioned unless referred to.

Signature: Mie Mohamed Mounir

Date: September 8th, 2020

Acknowledgments

Allah, thank you for all your countless blessings, and for enabling me to complete this work.

I would like to thank Dr. Andreas Kakargoukas, Assistant Professor of Cell and Molecular Biology, for his valued expertise, and guidance throughout the whole course of the lab work, proof reading and writing this thesis. I would like to extend my gratitude to Mr. Osama Said, and Mr. Amgad Ouf for their advice, help and support. I would like also to thank all my team members, and to extend my appreciation to my peers; Shimaa Farag, Alaa Yousef, Manar El Nagar, Amal Aboul Fetoh, Logyn Abushal, Haidy Amr, Shimaa Adel, Eric Zadok, Ahmed Safwat Abo Hashem, and Marwa Tawfiq to their tremendous support and aid. Also, I want thank AUC for funding this research.

To my dear friends Miral Ghanim, and Engie El-Sawaf, I could not have done it without your compassion, love, and empathy.

To my dear family, I will never be able to return even a small part of all the love, care, and encouragement that you always give me. Thank you.

Dedicated to my dear mother.

1. Introduction

Magnetite is an iron oxide mineral that is found innately on earth (Gieré, 2016), its common chemical name is ferrous-ferric oxide as it contains both Fe^{3+} and Fe^{2+} in its chemical structure ($\text{Fe}^{2+} \text{Fe}_2^{3+} \text{O}_4^{2-}$) (Könczöl et al., 2011). However, it is found to be part of the airborne combustion-derived nanoparticles (CDNP) in urban areas (Mesárošová et al., 2014). The desirable physical, chemical, and physiological compatibility of nanomaterials promoted their use in various industries (Donaldson et al., 2004). Iron oxide nanoparticles are in use in various fields; in medicine they are used as intravenous iron preparations, drug and gene delivery, and magnetic resonance contrasting agents, in agriculture as plant fertilizer and animal feed, and in environmental remediation of soil and water (Hadjipanayis et al., 2008; Nikonov et al., 2011; Sheykhbaglou et al., 2010; Zhang, 2003).

The presence of nanomaterials in various consumer products and being part of the airborne pollution; propose that the broad population will be exposed to those nanomaterials. Moreover, Inhaled nanoparticles can escape the lung and disseminate into the blood and other organs (Donaldson et al., 2004). The threat imposed by those particles is a factor of both their large surface area and the inherent reactivity and toxicity of their surface (Donaldson & Tran, 2002; Tran et al., 2000). The smaller the particle size, the larger surface area per unit mass of substance, so the toxicity of the substance will be accentuated (Donaldson et al., 2004). So, nanoparticles are more toxic than larger respirable particles (Oberdörster, 2000). Magnetite Nanoparticles induce oxidative stress through formation of reactive oxygen species, causing damaging effects to macromolecules (DNA, lipids, and proteins) (Wu et al., 2014).

Individuals with mutations in the gene coding for ATM (Ataxia telangiectasia mutated) kinase suffer from sensitivity to oxidative stress and reactive oxygen species (Cosentino et al., 2011). A-

T patients have an autosomal recessive disorder characterized with high predisposition to cancer, and radiosensitivity (Shiloh, 1997). Cells from A-T individuals exhibit failure to activate cell cycle check points. (Petrini, 2000; Shiloh, 1997). Therefore, A-T patients are predicted to have profound sensitivity to MNPs (Magnetite nanoparticles).

In this work we aim to reveal the role of ATM in the repair of DSBs associated with heterochromatin post exposure to MNPs, guided by the work of Goodarzi et al., 2008 and others, on the role of ATM in repair of heterochromatin post IR (Ionizing radiation). Also, to demonstrate any differences in the genotoxicity and the repair kinetics post MNPs than IR. To demonstrate if there is any significance of ATM in managing the repair in the highly compacted heterochromatin post MNPs, and that not only ATM's role is restricted to managing oxidative stress, and cell cycle check points activation.

2. Literature Review.

2.1 Magnetite nanoparticles as an industrial biological hazard.

Magnetite nanoparticles (MNP) have been part of the particulate matter in air in urban areas; specially in underground stations (Johansson & Johansson, 2003) and welding workplaces (Sowards et al., 2008). Ultrafine particulate (< 100 nm) matter in air have been a rising concern due to their high surface area to mass ratio. The hazardous effect of these materials increase as their surface area increases.

Large cities like Cairo, New Delhi, and Kathmandu usually have high concentration of particulate matter smaller than 10 μm (PM_{10}); around 300 $\mu\text{g}/\text{m}^3$ or even higher (Grobety et al., 2010). While the World health organization (WHO) guidelines for air quality that states that PM_{10} should not exceed 20 $\mu\text{g}/\text{m}^3$ annually or 50 $\mu\text{g}/\text{m}^3$ per day. Residents of those cities inhale daily those hazardous particulate matter with every breath.

Nanomaterials penetrates body tissues quite easily; they can infiltrate through vascular endothelium, olfactory nerve, alveolar capillary, olfactory and blood brain barrier (BBB) (Calderón-Garcidueñas et al., 2016, 2017; González-Maciel et al., 2017; Maher et al., 2016). As they are characterized by their nano-size, and large surface area that renders them quite bioreactive and accessible to internal tissues, cells and subcellular structures.

In 2016, 37 human brain samples were collected and analyzed from cadaver brains from Manchester city, UK, and Mexico City. These samples showed the presence of Magnetite nanospheres identical to Magnetite nanospheres formed from combustion and found in air particulate matter, these nanospheres were structurally distinct from endogenously formed cubohedral magnetite nanoparticles (Maher et al., 2016). These combustion derived nanoparticles

were present at concentrations fluctuating between 0.2-12 $\mu\text{g/g}$ dry tissue. Sizes of these nanospheres ranged from 10-150 nm

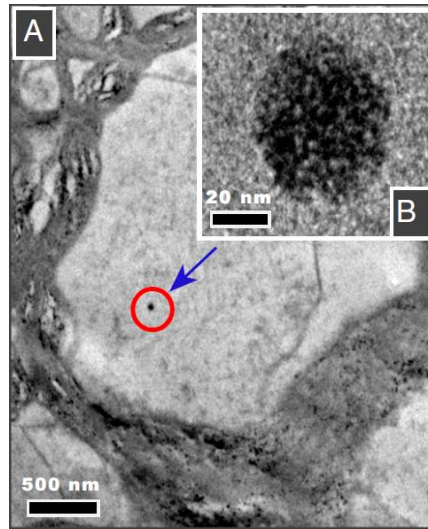


Figure 1 Transmission electron micrograph of thin brain sections.

A) Showing the presence of Magnetite nanospheres present in frontal brain cells. B) A higher magnification demonstrating the Magnetite nanospheres that are identical to Magnetite nanospheres produced from combustion (Figure adapted from Maher et al., 2016).

The presence of these combustion derived magnetite nanoparticles in human brains have been strongly associated with neurodegenerative disorders specially Alzheimer's disease (Maher et al., 2016). MNPs was found to be deposited in human hearts of residents of Mexico City, after daily exposure to high levels of PM exceeding the National Air Ambient Quality Standards for the United States. The deposition of the MNP in the cardiac muscle was linked to increased incidence of CVS disease and mortality (Calderón-Garcidueñas et al., 2019).

2.2. Role of reactive oxygen species in Magnetite Nanoparticles genotoxicity

Magnetite nanoparticles impart oxidative stress on cells as they generate reactive oxygen species (ROS) through different pathways. The production of ROS happens at the surface of the nanoparticles rather than from the iron ions released into solution (Voinov et al., 2011). Hydroxyl radicals are produced from the Fenton reaction upon decomposition of hydrogen peroxide in presence of iron ions (Voinov et al., 2011).



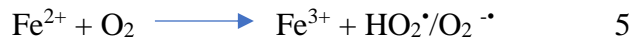
Hydroxyl radicals are also generated by another superoxide driven Fenton reactions called Haber-Weiss reactions.



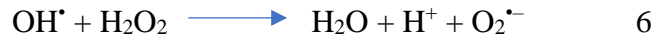
MNPs contains Fe^{2+} and Fe^{3+} at the surface with a ratio around 1:2.6 (confirmed by X-ray photoelectron spectroscopy) (Voinov et al., 2011). The Superoxide anion and the hydrogen peroxide are produced physiologically in intracellular and extracellular compartments from activated phagocytes (Babior & Woodman, 1990), lymphocytes (Maly, 1990), fibroblasts (Murrell et al., 1990), and endothelial cells (Babbs et al., 1991), in addition to the electrons that escape from the electron transport chain (Fridovich, 1989).

Also, ferrous ions can react with molecular oxygen to produce free radicals or ferryl-oxo complexes.





Additionally, these reactions may take place (Valko et al., 2005):



Oxidative damage to the DNA is diverse; they include single and double strand breaks and single base modification 8-hydroxy deoxyguanosine (8-OH-dg) (Sonmez et al., 2016) and thymine glycol (Evans et al., 1993). Iron ions in the cytosol released from enzymatic lysosomal degradation, produce highly reactive hydroxyl radicals.

2.3 Ataxia Telangiectasia disorder, DNA double strand breaks and DNA repair.

Ataxia telangiectasia (A-T) disorder is an autosomal recessive disorder that occurs due to mutations in the ATM (Ataxia telangiectasia mutated) protein (Thomas O. Crawford, 1998). It is commonly called the DNA damage response or genome instability syndrome. The disease is characterized with progressive ataxia, oculocutaneous telangiectasia, cerebellar degeneration, radiosensitivity, increased incidence of cancers specially cancers of lymphoid origin, recurrent sinopulmonary infections and premature aging. Other anomalies include growth retardation, delayed puberty, gonadal atrophy, and diabetes (Nissenkorn et al., 2016). Not all A-T patients have all the same consistent set of symptoms and/or laboratory findings. The incidence of A-T is 1:40,000 to 1:100,000 and in some populations it is as uncommon as 1:300,000 (Riboldi et al., 2020). Life expectancy in A-T patients is markedly reduced, and was reported to be 25 years in 2006 (Crawford et al., 2006).

A-T disease develops due to mutations in ATM gene as previously mentioned; Missense, Non-sense, frame shift, insertion-deletion mutations have been reported. Also, mutations in ATM alleles may be compound heterozygous mutations. All these mutations result in a truncated nonfunctioning ATM protein (Reviewed in Riboldi et al., 2020) .

ATM, one of the phosphoinositide 3-kinase (PI3K)-related kinase (PIKKs) that phosphorylates a lot of downstream targets like chk1/2, p53, and H2AX (Blackford & Jackson, 2017). ATM is responsible controls different cellular functions; as DNA repair, cell cycle check points control, and protects the cell from exogenous toxic insults (Oxidative damage, alkylating agents, and ionizing radiations. Loss of functioning ATM protein results in the inability of the cells to repair DNA damage, resulting in increased cancer incidence and radiosensitivity (Zaki-Dizaji et al., 2017). ATM is also known for production of immunoglobulins and responsible for lymphoid cell survival. Therefore, A-T patients have higher incidence of cancers of lymphoid origin and autoimmune diseases (Reviewed in Riboldi et al., 2020).

So, the inability of the cells to preform proper repair of the DNA damage that happens due to the absence of a functioning ATM protein leads to a higher cancer incidence and marked radiosensitivity among A-T patients (Rothblum-Oviatt et al., 2016). The deleterious damage might arise from a single point mutation to a chromosomal aberration. One of the most deleterious DNA lesions is Double Strand Breaks (DSBs), it is of utmost importance that DSBs are repaired in a high-fidelity manner. On formation of double strand breaks ATM protein abundant in the nucleus gets activated an auto phosphorylated at S 1981, and starts the phosphorylation of downstream targets (Bakkenist & Kastan, 2003).

2.4. Role of Ataxia Telangiectasia Mutated in DNA double strand breaks repair.

ATM is one of the phosphatidylinositol kinases involved in DNA damage repair mechanism (Czornak et al., 2008). They initiate the DNA repair mechanism by activating cell cycle checkpoints, diversion of transcription, or initiation of apoptosis in case of failure of the repair process (Figure 2).

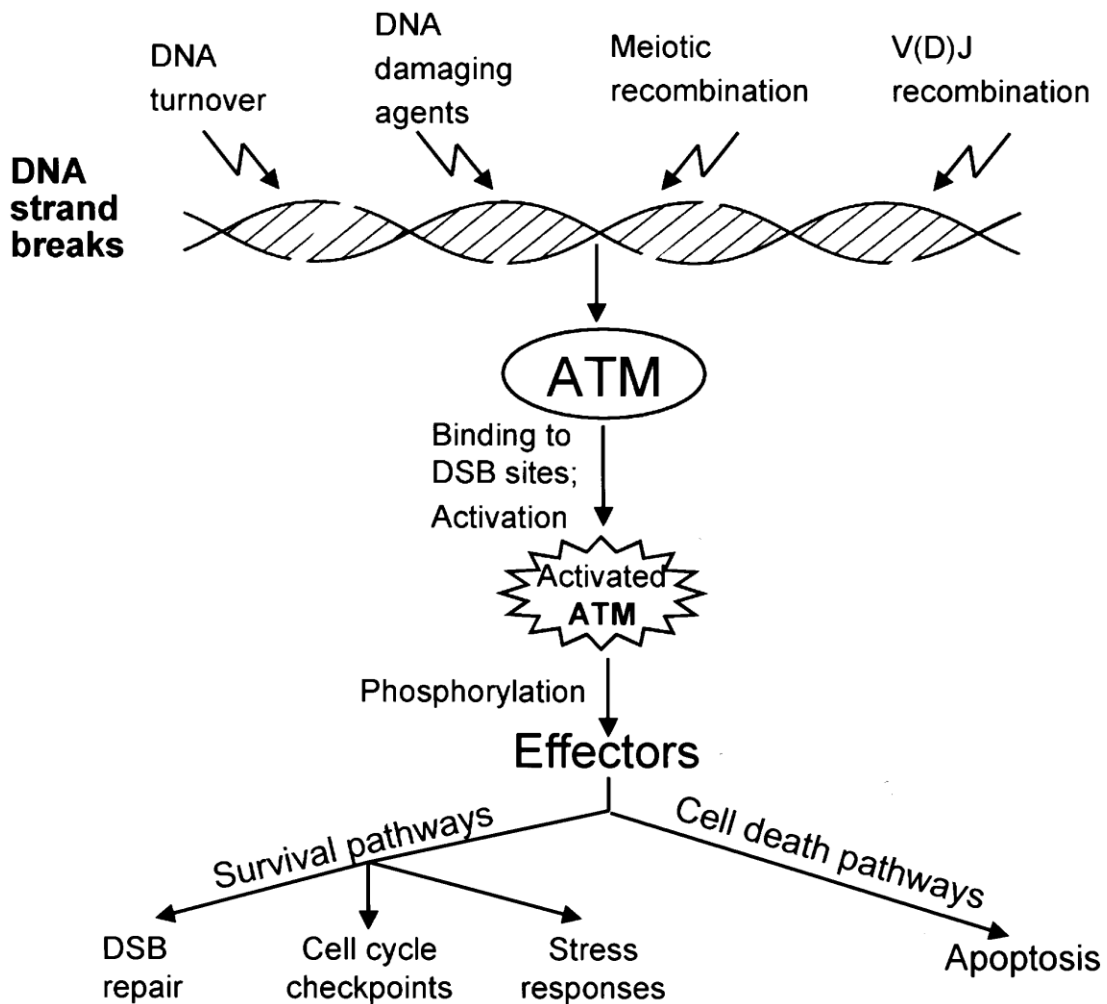


Figure 2 ATM response to DNA double strand breaks.

ATM phosphorylates a great deal of substrates to promote DNA repair and cellular survival, and when the DNA damage is irreparable it induces the apoptotic pathway (Figure adapted from Barzilai, 2002).

ATM, DNA-PKcs, and ATR are PIKKs. They all have N-terminal HEAT (Huntingtin, elongation factor 3, a subset of protein phosphatase 2A, TOR1) repeats domain that arbitrate interactions with other proteins. Their C-terminal contains the kinase domain and PIKK regulatory domain flanked by a FAT (FRAP-ATM-TRRAP) and FAT-C motif (Figure 3).

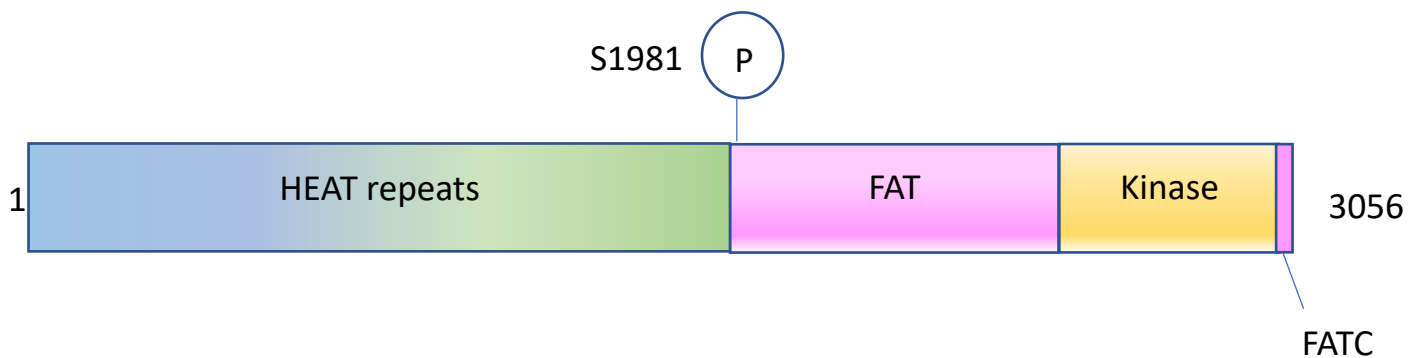


Figure 3 Structural model for ATM.

Protein domains (Heat repeats, FAT, Kinase, and FATC domains) are shown as colored boxes. Numbers indicate amino acids. Encircled P indicates commonly phosphorylated site. Figure Adapted from (Blackford & Jackson, 2017).

ATM functions by phosphorylating their protein substrates at serine or threonine molecules that are followed by glutamine (SQ or TQ motif) (S.-T. Kim et al., 1999; O'Neill et al., 2000). Generally, for ATM, ATR and DNA PKcs they phosphorylate SQ or TQ motifs that are flanked by hydrophobic or acidic residues. While the presence basic residues in their proximity tends to

be a negative determinant for phosphorylation (Bannister et al., 1993; Chen et al., 1991; Lees-Miller & Anderson, 1989).

ATM is a nuclear protein, whose expression level isn't changed when exposed to ionizing radiation while the protein kinase activity has a 2-3 fold increase (Kurz & Lees-Miller, 2004). Phosphorylation of 1981 serine found in ATM amino-terminal FAT domain was found to be essential for ATM induced phosphorylation of p53 and cell cycle check points activation. Transphosphorylation and dissociation of ATM from an inactive dimeric form to active monomer is essential for the activation of ATM (Bakkenist & Kastan, 2003).

When double strand breaks are formed the MRN complex (Mre11, Rad50 and NBN) is recruited first to the site. Mre11 starts with the end processing, then ATM is activated through autophosphorylation and monomerization. The activated ATM recruited at the site of DNA DSB (Double Strand Break) is then released to initiate phosphorylation of more distant substrates as the histone variant H2AX (Bakkenist & Kastan, 2003; Rogakou et al., 1999). Also, p53 BP1 (Binding protein 1) and MDC1 (Mediator of DNA damage check point 1) are involved in ATM activation (Blackford & Jackson, 2017). However, BRCA1 isn't involved in the activation of ATM, it is required for the phosphorylation of ATM downstream targets such as p53, NBN, c-jun and Chk2 (Foray, 2003).

ATM activation results in direct or indirect phosphorylation of a lot of downstream targets. It is a working process to identify which of those are functionally important in the DNA repair mechanism. Most of the substrates that are phosphorylated by ATM, are phosphorylated by ATR as well, while others such as H2AX are phosphorylated by DNA-PKcs instead. ATM directly phosphorylates p53 at serine 15 and H2AX at serine 139, others are phosphorylated by ATM-arbitrated regulation of protein kinases as Chk1, Chk2 (Yosef Shiloh, 2003), and others c-abl and

cdk1 cdk2. Phosphorylation of p53 serine15 is mitigated and delayed in A-T cells, but still phosphorylation at serine 15 happens later post IR which indicates that ATM is responsible for the early phosphorylation of S15 while later it can be compensated by other kinases as ATR (Siliciano et al., 1997). Also, IR induces phosphorylation of p53 at serines 6, 9, 20, 33, 46, 315, and 392. ATM induces phosphorylation of 9, 20, 46 as well as 15. However, phosphorylation of S20 and 46 is more dependent on ATM than S15 (Saito et al., 2002).

The Majority of DNA repair is ATM independent, but the loss of ATM or any of the downstream proteins causes 10-25% repair defect in non-dividing cells (Goodarzi et al., 2008). So, any mutation in ATM confers severe radiosensitivity.

2.5 Ataxia Telangiectasia Mutated activation by oxidative stress.

An alternative form of active ATM in response to oxidative stress was described by (Guo et al., 2010), distinct from in response to double strand breaks. ATM activated through oxidative stress, is an active disulphide cross-linked dimer (Guo et al., 2010), unlike the active monomer that is activated through the MRN complex in response to DSBs. ATM activated by oxidative stress did not phosphorylate H2AX and Kap-1, in contrast to ATM activated through MRN. However, they activated P53 and Chk 2 as ATM activated through DSBs and MRN (Guo et al., 2010). N-acetyl cysteine (Antioxidant) blocked the phosphorylation of P53 and Chk2 in response to H₂O₂ (Oxidative stress), while it did not affect the phosphorylation of P53 and Chk2 in response to DSBs produced from bleomycin. S 2991 found in FAT-C domain was found to be involved in the formation of the ATM disulphide cross linked dimer.

Since the magnetite nanoparticles introduce DNA damage in response to formation of ROS. So, it would be predicted that a fraction of ATM expressed in the cells would be activated by producing the disulphide cross linked dimer, resulting in the phosphorylation of P53, Chk2 but not KAP-1 or H2AX.

Moreover, ATM activation due to oxidative stress activates the pentose phosphate pathway (PPP) (Cosentino et al., 2011), increasing the activity of glucose 6-phosphate dehydrogenase (G6PD), resulting in increasing NADPH. NADP is a cofactor of glutathione reductase and cytochrome p450 reductase that contributes to regulating the cellular redox balance. Therefore, Cells lacking ATM has been shown to have high levels of reactive oxygen species (ROS), and they are sensitive to drugs that induce oxidative stress (Barzilai, 2002).

2.6 Factors controlling heterochromatinization.

Chromatin can be generally distinguished into euchromatin (Eu “true”) and heterochromatin (hetero “different from true chromatin”). Heterochromatin is the more compacted portion of the DNA; that is either constitutively or transiently silent. The centromeric, telomeric chromosomal ends, and pericentromeric satellite DNA compose the constitutively silent portion of heterochromatin that remain condensed throughout the cell cycle (Revised in Craig, 2005). The transiently silent (Facultative heterochromatin) portions of the heterochromatin are found within euchromatin and is usually silenced during aging and development (Brockdorff, 2002). While Euchromatin is the more relaxed, actively transcribed portion of the DNA. Heterochromatin was shown to have an impact on DNA repair as much it does on other nuclear processes such as transcription and replication.

Heterochromatinization is controlled by many factors including regulators of histone acetylation and methylation, sequence specific repressors and corepressors, chromodomain adaptor proteins that frequently bind to methylated histones, proteins involved in DNA methylation and nucleosome remodeling enzymes (Figure 4) (Craig, 2005).

The mechanism and the sequence by which the heterochromatin proteins are assembled to compact chromatin have been thoroughly studied. One of the mechanisms starts with transcriptional repressors binding to the DNA in a sequence specific manner (Figure 4). They bind through DNA binding motifs; most commonly zinc fingers (Urnov, 2002) that binds to 3 base pairs on a DNA strand. These DNA binding motifs occur in tandems to allow the repression of a wide range of DNA sequences. Transcriptional corepressors then bind to the repressors to assemble other heterochromatinization factors. Corepressors can be a part of or associate with macromolecules with Histone deacetylase activity (Ahringer, 2000). Histone deacetylases (HDACs) are one of the core components of heterochromatinization. They can be recruited by either repressors, corepressors, or proteins that binds to methylated DNA. Histone deacetylases can be targeted to newly deposited histones after DNA replication to remove acetyl groups from suitable residues. HDACs can form homodimers, heterodimers, can join other heterochromatinization proteins, or form macromolecular complexes with heterochromatin components usually with ATM dependent chromatin remodellers.

After eviction of the acetyl groups from histones, begins the role of Histone methyl transferases HMT. All HMT associated with repression contains a SET domain (named after three drosophila histone methyl transferases: Suv (Var) 3-9, Enhancer of zeste, Trithorax). H3-K9, H3-K27, and H4-K20 are the lysine residues on histones when methylated promotes repression. These lysine

residues can carry from 1 to 3 methyl groups; so HMT enzymes can modify the same lysine residue more than once (Sims et al., 2003).

H3-K9 methylation is mediated by Suv39h1 and Suv39h2 that is involved in compaction of the pericentric regions (Peters et al., 2001) and genomic imprinting (Fournier et al., 2002), it is also found at the promoters of silences genes. H3-K27 trimethylation is mediated by Enhancer of zeste EZH2 also known in mouse as Enx1, it also can trimethylate H3-K9. H3-K27 trimethylation and H3-K9 dimethylation mediated by EZH2 is involved in silencing of mammalian Xi (Plath et al., 2003). Monomethylation and trimethylation of H4-K20 is mediated by PR-Set7 (Cao et al., 2002) and Suv4-20h1/2 (Kourmouli et al., 2004) respectively.

HP1 and polycomb are adaptor proteins that aid in formation of macromolecular complexes with heterochromatinization proteins. HP1 interacts with methylated histones and HMTs to ensure chromatin compaction (Lachner et al., 2001); an example for this is the binding of HP1, Suv39h, and H3K9. Usually that trio HP1/HMT/methylated lysine is found at the core of all heterochromatic regions. Polycomb group proteins (PcG) repressor proteins have a chromodomain that interacts with corepressors, HDACs and chromatin remodeling proteins (van der Vlag & Otte, 1999).

DNA methyl transferase (DNMTs) methylate CpG nucleotides. There are De novo methyl transferase and maintenance methyl transferase; DNMT 3A/B and DNMT1, respectively. In early embryogenesis DNMT 3A/B is highly expressed to start the wave of De novo methylation (Meehan, 2003). Methyl CpG binding proteins (MeCPs) from their name they are proteins that have methyl CpG binding domains, they compete with trans activating proteins (Wade, 2001). MeCP2 and MBD1/2 are the major methyl CpG binding proteins. They also have domains to recruit other factors of heterochromatinization like HDACs, corepressors and ATP dependent

chromatin remodeller (Wade, 2001). ATP chromatin remodellers use the energy from hydrolysis of ATP to loosen the interaction between DNA and histones noncovalently to allow the work of the heterochromatinization factors (Ahringer, 2000).

Despite the presence of similar factors at the heterochromatic loci, there's no one pathway to achieve heterochromatinization (Craig, 2005).

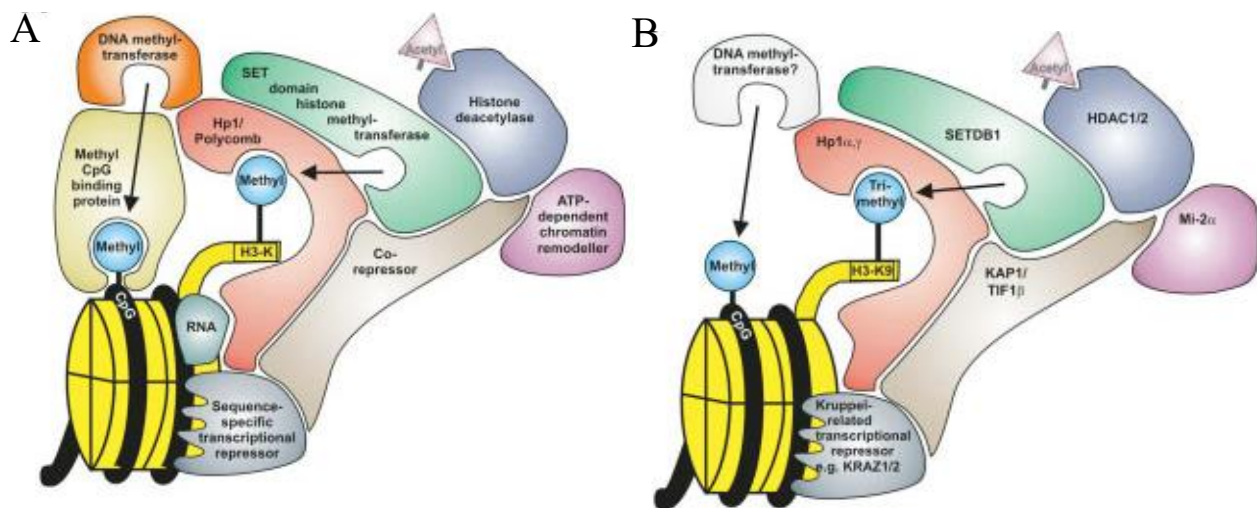


Figure 4 Diagram showing heterochromatinization pathway.

A) General heterochromatinization pathway. Sequence specific transcriptional repressor binds to a certain sequence in the DNA. Then a corepressor and/or HP1/polycomb gets recruited by the repressor. Afterwards the corepressor recruits a chromatin remodeller that loosens the binding between DNA and histones on the nucleosome. HDACs that removes an acetyl group from lysine residue on H3/H4 tail. Then SET HMT gets recruited to add a methyl group on the same tail of H3. SET HMT and methylated lysine group recruits HP1/polycomb, that recruits DNA methyltransferase that adds a methyl group to CpG residues. Afterwards methyl CpG binding proteins binds to the methylated CpG residues. B) Factors assembled by Krüppel associated box repressor (Figure adapted from (Craig, 2005)).

2.7 Ataxia Telangiectasia Mutated and chromatin modulation post ionizing radiation.

The ATM DSB repair fraction comprises about 10-25% of DSBs; for γ induced radiation DSBs it makes up about 10-15%, while for α -particles it comprises 20-25% (Riballo et al., 2004). So, it was thought that the involvement of ATM in the repair process is related to damage complexity. However, later it was attributed to relaxation of heterochromatin to initiate the repair process, as the ATM dependent repair fraction never exceeded 25% in spite of damage complexity (Goodarzi et al., 2008).

On formation of DNA damage, an important requirement for DNA repair is the accessibility of the damaged sites. Higher order chromatin structure poses an obstruction for the accessibility of the DNA repair machinery to the damaged sites. Consequently, the relaxation and recompaction of heterochromatin must be precise and efficient. ATM was involved in the relaxation of heterochromatin post IR, through phosphorylation of the transcriptional corepressor KAP-1 (Goodarzi et al., 2009).

KAP-1 is an obligate corepressor (Figure 5) that binds to the Krüppel associated box zinc finger protein (KRAB ZFP). The KRAB ZFPs are repressors that binds to the DNA through their zinc fingers (White et al., 2012). KAP-1 binding to KRAB ZFP promotes heterochromatinization through being an anchor for the gathering of gene silencing proteins; HP1, H3-K9 methyltransferase Su(var)3-9, chromatin remodeling factor Chromodomain helicase DNA-binding protein 3 (CHD3/Mi-2a), and enhancer of zeste domain protein 1 (SETDB1) (Ayyanathan et al., 2003; Lechner et al., 2000; Schultz et al., 2001, 2002).

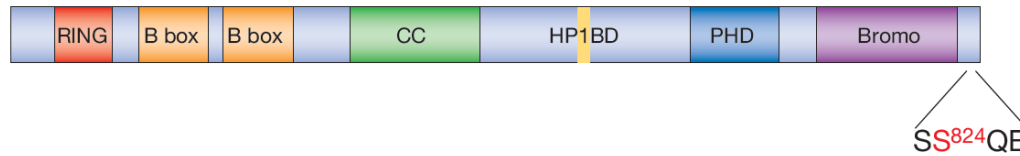


Figure 5 Schematic diagram for KAP-1 domains.

KAP-1 possesses a tripartite motif composed of Ring, B1 box, B2 Box, and coiled coil (RBCC domain). This Tripartite motif enables KAP-1 to bind to KRAB domain. HP1BD is the domain that binds to HP1. ATM's target S824 is found at the carboxy terminus.

Post IR DNA damage associated with heterochromatin has been known to be repaired more slowly than euchromatin (Huisinga et al., 2006). As Heterochromatin hinders the progression of ATM mediated phosphorylation of H2AX (J.-A. Kim et al., 2007). ATM was shown to be involved in the relaxation of heterochromatin post IR, as it phosphorylates KAP-1 at S 824. Also, KAP-1 gets phosphorylated at the G1/S interphase at S 473, S 473 phosphorylation happened later than the phosphorylation of S 824, however S 473 was not dependent on S 824 phosphorylation (White et al., 2012). Regulation of the phosphorylation of both S 824 and S 473 was done by HP 1 (White et al., 2012). On induction of DSBs post IR pan nuclear phosphorylation of KAP-1 happens, that gets resolved within hours. However, pKAP-1 (Phosphorylated Kap-1 at S 824) signal remains persisting at the sites of the slowly repairing DSBs of heterochromatin (Noon et al., 2010). This pan nuclear phosphorylation of KAP-1 occurs due to the abundance of activated ATM throughout the nucleus, that gets concentrated at the sites of DSBs by the action of MRN, 53BP1, MDC1, RNF8, and RNF168 (Goodarzi et al., 2009). Cells deficient in 53BP1, manifested a DSBs repair defect in HC identical to cells lacking ATM, This is attributed to the fact that ATM failed to be concentrated at the sites of DSBs due to the lacking 53BP1 (Noon et al., 2010). Knockout of KAP-1 and expression of constitutively phosphorylated KAP-1 (KAP-1^{S824D}) abolish the requirement of

ATM in HC repair. While expression of KAP-1^{S824A} mutant that inhibit the phosphorylation at S824, caused a persisting repair defect in HC even in presence of ATM (Goodarzi et al., 2008).

ATM merely caused relaxation of the heterochromatin structure rather than dismantling of the heterochromatin structure (Goodarzi et al., 2009) as there was no drastic changes noticeable in the heterochromatic structure, and on phosphorylation of KAP-1 it remained bound to the DNA. No Difference happened in the physical association of KAP-1 within the nucleosomes, or difference in the interaction between KAP-1 and other heterochromatinization proteins like HP1 or HDAC1/2 (Goodarzi et al., 2008; Noon et al., 2010; Ziv et al., 2006). Only transient relaxation of the compaction of nucleosomes were detectable; that caused them to be nuclease digestible in vitro (Ziv et al., 2006). Moreover, the phosphorylation of KAP-1 prevents its auto-SUMOylation. That is necessary for interaction with SETDB histone methyl transferase and CHD3/mi-2 α chromatin remodelling enzyme (Ivanov et al., 2007).

The DNA damage response that happens in the HC associated DSBs requires ATM associated mediators such as MDC1, 53BP and the nuclease Artemis. Artemis deficient cells had no difference in phosphorylation of KAP-1 in HC DSBs, however they showed a marked defect in repair of those HC DSBs showing that Artemis acts downstream of the pKAP-1 (Goodarzi et al., 2010).

3. Aim of Work.

3.1 Monitoring the repair kinetics of DNA double strand breaks associated with heterochromatin and euchromatin post exposure to Magnetite nanoparticles.

In this work we aim to investigate the total DNA repair kinetics; and the repair of the DSBs associated with heterochromatin and euchromatin post exposure to MNPs. The tightly compacted fraction of chromatin was shown to have slower repair kinetics when subjected to ionizing radiation (Goodarzi et al., 2008), we want to observe if that is the case with MNPs induced damage. We aim to monitor if there are any visible changes in the superstructures of the chromocenters on repairing the heterochromatin associated double strand breaks. Also, we want to determine the percentage of heterochromatin associated DSBs and whether it comply with the percentage of DSBs that require ATM for repair.

3.2 Revealing of the mechanism required for the repair of heterochromatin associated DNA double strand breaks post Magnetite nanoparticles exposure.

We want to reveal the role of ATM post exposure to MNP; in the repair of the heterochromatin associated DSBs. And whether the mechanism of repair of the heterochromatin associated DSBs post IR utilizing ATM, is also followed post MNPs exposure. So, on inhibition of ATM we want to observe if the heterochromatin DSBs repair is affected, and if there would be any persistence of γ -H2AX around the heterochromatic chromocenters.

3.3 Evaluation and comparison of the repair mechanisms required for the repair of heterochromatin associated DNA double strand breaks post Magnetite nanoparticles and Neocarzinostatin exposure.

We will compare and evaluate the repair kinetics of heterochromatin associated DSBs on inhibition of ATM post exposure to MNP and NCS. The comparison of our kinetics results with NCS; will uncover if the proposed by Goodarzi et al., 2008 in the involvement of ATM in the transient relaxation of heterochromatin is comparable with MNP.

4. Materials and Methods

4.1 Cell line

L929 murine adherent fibroblasts obtained from subcutaneous connective tissue; areolar and adipose tissue of C3H/An mouse. L929 murine cell line possesses an acrocentric nucleus. On staining the nuclei with DAPI (4',6-diamidino-2-phenylindole) centromeric and pericentric regions (heterochromatin) appears to be stained more densely. These densely stained regions were shown to have enrichment in the markers of heterochromatinization such as KAP-1, HP1, CENP-A (Centromeric protein A), H3K9 me3 (Histone 3 trimethylated at Lys9) (Figure 6). In addition to the absence of euchromatic markers HMGB1 (High mobility group protein B1) and transcription factor E2F1 (Goodarzi et al., 2009). Therefore, investigation of DNA repair in heterochromatin was feasible.

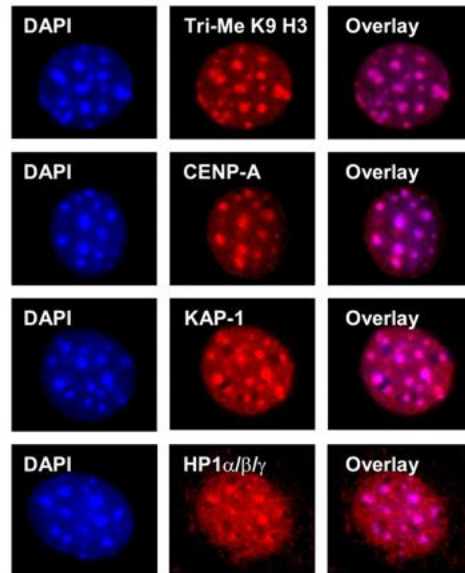


Figure 6 Localization of heterochromatic markers H3K9me3, CENP-A, KAP-1, and HP1.

Heterochromatic markers (H3K9me3, CENP-A, KAP-1, and HP1) are shown to be enriched in the chromocentres (Densely stained DAPI regions) (Figure adapted from Goodarzi et al., 2008)

4.2 Chemicals and nanoparticles.

All the following was obtained from Sigma Aldrich. Iron (II), (III) oxide nanopowder (637106), having 50-100 nm particle size (SEM), 97% trace metals basis (including Mg, Al, Mn and Ti (Dare et al., 2014; Müller et al., 2003)) . Neocarzinostatin from *Streptomyces carzinostaticus* (N9162). ATM inhibitor (ATMi) KU55933 (SML1109).

4.3 Nanoparticles Dispersion.

Magnetite Nanoparticles were suspended in fresh Dulbecco's Modified Eagle Medium (DMEM) at concentration of 100 µg/ml. The nanoparticles were dispersed before treatment using QSonica, Q700, Sonicator with high power probe sonication in pulsed mode (1s on/1s off), for 20 minutes to ensure homogenous suspension (Könczöl et al., 2011). Then diluted in fresh media as needed.

4.4 Cell Culturing.

L929 cell line was cultured in fresh Dulbecco's Modified Eagle Medium (DMEM) containing 4.5 g/L glucose, with 2 mM L-glutamin, 10% (v/v) fetal bovine serum (FBS) and penicillin/streptomycin (50 IU/ml and 50 mg/ml, respectively). The cells were incubated at 37°C in humidified 95 % and 5% CO₂ air. The cells were passaged when they reached 90 % confluency.

4.5 Immunostaining technique.

Cells attached on coverslips (18*18mm) are fixed with 4% formaldehyde for 30 minutes. Then washed twice with phosphate buffer saline (PBS). Afterwards 0.2% triton is added for 3 minutes, then washed three times with PBS. Next the cells are blocked with 5% bovine serum albumin (BSA) for 30 minutes. Then the primary antibody; anti-γH2AX (Ser139) (Merck Millipore, 05-636) (diluted in 5% BSA 1:600) is added for 1 hour. Consequently, the coverslips were washed three times with PBS, then chicken anti-mouse secondary antibody Alexafluor488 (Thermofisher

scientific, A21200) (diluted in 5% BSA 1:200) is added for 1 hour in dark (Kawanishi et al., 2013). Finally, the nuclei were stained with 5 $\mu\text{g/ml}$ DAPI (4',6-diamidino-2-phenylindole) for 10 minutes, then washed three times with PBS. The coverslips then are mounted on Fluoroshield mounting media (Thermofisher scientific, F6182-20ML) on microscope slides. The slides were examined by Leica DM 2000 fluorescent microscope.

4.6 Dose response of Magnetite nanoparticles in L929 cell line.

L929 cells were seeded at a density of (6×10^5) per well in a 6-well plate and left overnight for attachment. Then increasing concentrations of MNPs were added (0.1, 1, 5, 10, 20 $\mu\text{g/ml}$) for 24 hours (Kawanishi et al., 2013). A control coverslip is done without addition of MNPs. All coverslips were stained and fixed according to the method explained in 4.5 Immunostaining technique. Then the slides were examined by Leica DM 2000 fluorescent microscope. Images taken were adjusted and cropped by ImageView and Fiji software.

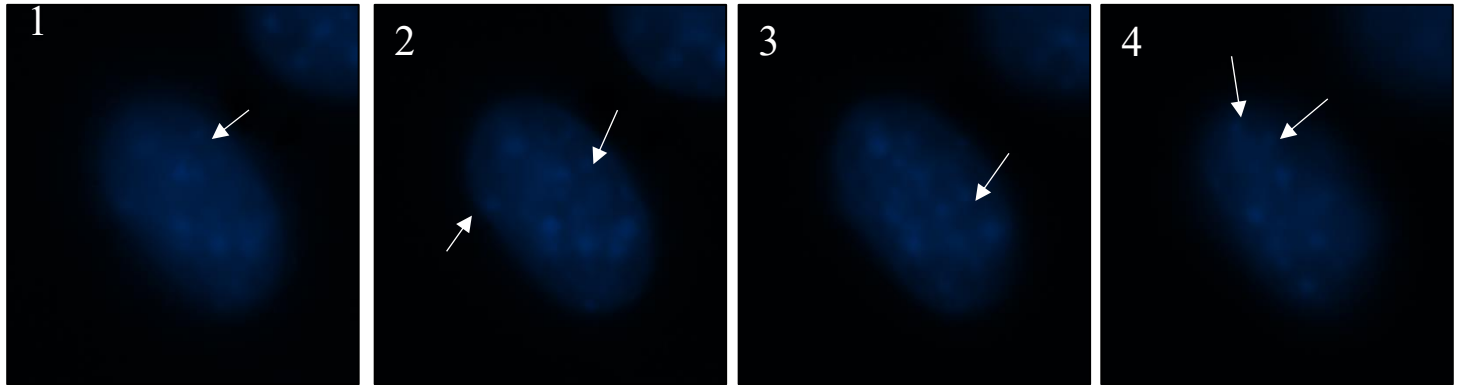
4.7 Assessment of DNA damage repair associated with heterochromatin after exposure to MNP.

DNA damage repair is assessed by monitoring the resolution of DNA damage repair foci that are present at the site of DNA DSBs. Phosphorylation of H2AX ($\gamma\text{-H2AX}$) is one of the earliest events in DSBs recognition and repair (Pilch et al., 2003). Sites of double strand breaks are visualized by immuno-staining with antibodies against the phosphorylated histones ($\gamma\text{-H2AX}$) (Thoroughly explained in 4.5 Immunostaining technique.)

L929 cells were seeded on coverslips at a density of (6×10^5) per well in a 6-well plate, then allowed to attach overnight. Cells are seeded in high density to be contact inhibited (G1 phase) on the day of the experiment. Then 5 $\mu\text{g/ml}$ of MNP are added for 24 hours. Afterwards, fresh media is added to remove the nanoparticles and allow the cells to repair. The cells are fixed at different time points of repair (0.5, 2, 5, 16, and 24 hours) (Goodarzi et al., 2008). A control coverslip is done without MNP treatment and fixed after 24 hours of fresh media. Then the cells are stained with anti- γH2AX (Ser139) (Merck Millipore, 05-636), anti-mouse secondary antibody Alexafluor488 (Thermofisher scientific, A21200), and DAPI (details of fixation and immunostaining in 4.5 Immunostaining technique). The slides are examined by Leica DM 2000 fluorescent microscope. The DAPI stained nuclei are seen under 340-380 nm excitation, the DNA damage foci are seen through 450-490 nm excitation.

Throughout the cell cycle heterochromatin remains visibly condensed (Huisinga et al., 2006). So, regions of heterochromatin can be easily identified on staining with DAPI, as they appear as densely stained regions within the nuclei of the acrocentric murine cell line L929. Multiple images are taken for the nuclei stained with DAPI at different planes (Figure 7), to capture all of the densely stained regions of heterochromatin found on these different planes. Then multiple images are taken for $\gamma\text{-H2AX}$ foci as well (Figure 9). All the DAPI images are merged into one image with all the Heterochromatin blobs (Figure 7) using the color composite tool on ImageView software, and the same is done for the $\gamma\text{-H2AX}$ foci images (Figure 9). Subsequently, both the overlaid images of DAPI and $\gamma\text{-H2AX}$ foci are overlaid (Figure 11). Images are cropped using Fiji Software.

A



B

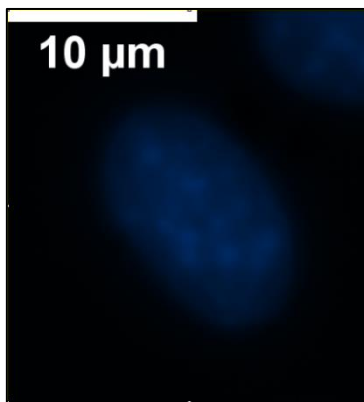


Figure 7 L929 nucleus stained with DAPI, showing densely stained regions of heterochromatin.

A) Images from 1 to 4 are images of the same nucleus taken at different planes to see all heterochromatin densely stained regions (Arrows). B) Merged image for all planes showing the DAPI densely stained regions.

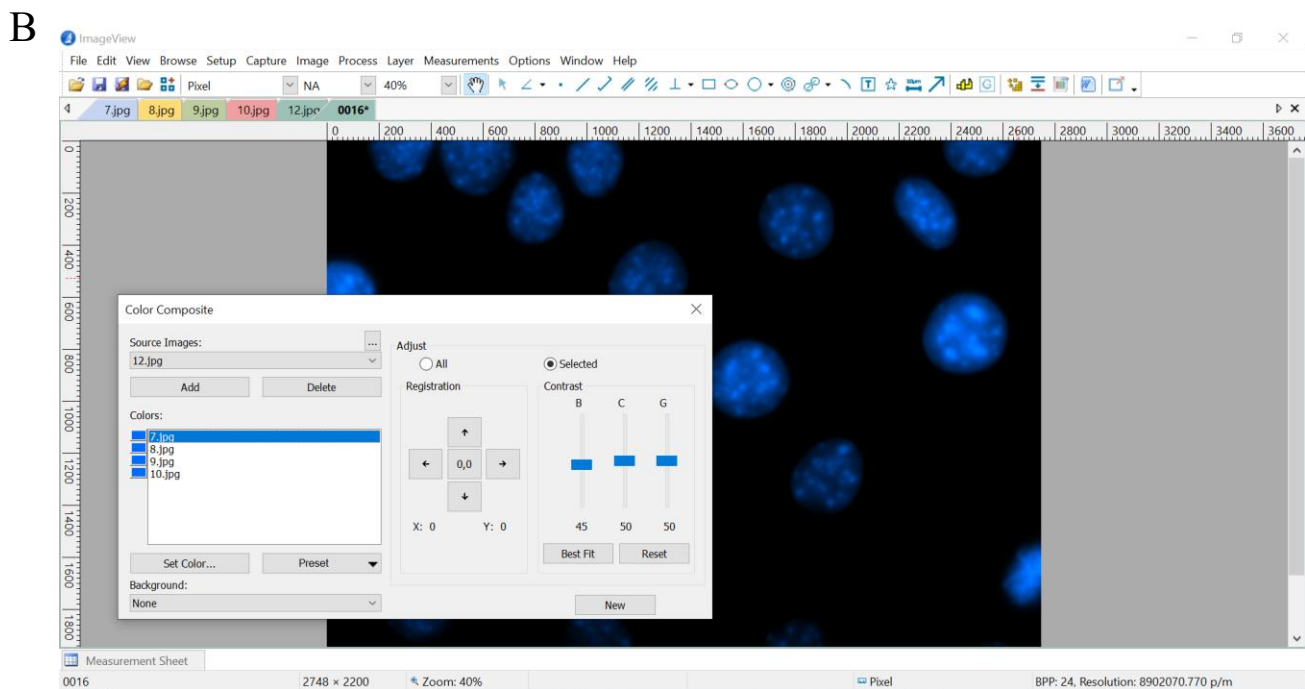
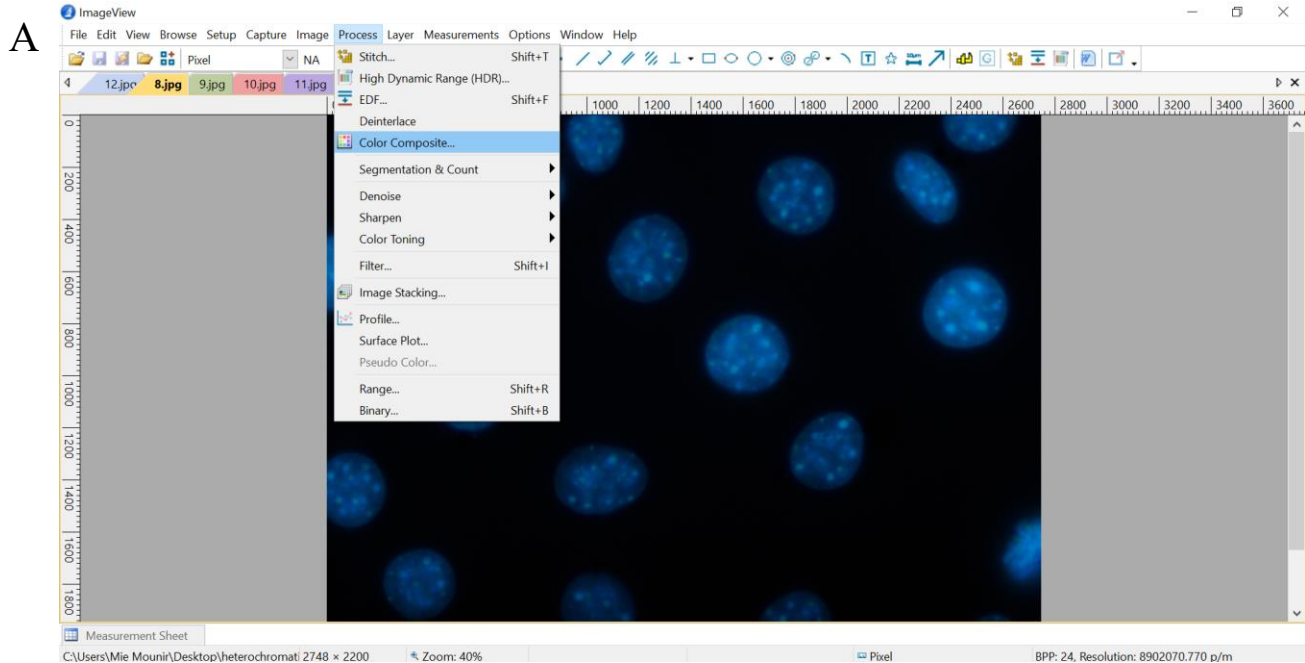


Figure 8 Screen shots showing the use of color composite tool on Imageview software to collate all DAPI images into one.

To assess the DNA repair of DSBs correlated with heterochromatin, for each time point total number of γ -H2AX foci per cell is counted from the merged γ -H2AX foci images (Figure 9). Then

the number of γ -H2AX foci associated with heterochromatin is counted from the merged images of γ -H2AX foci with the DAPI (Figure 11.3).

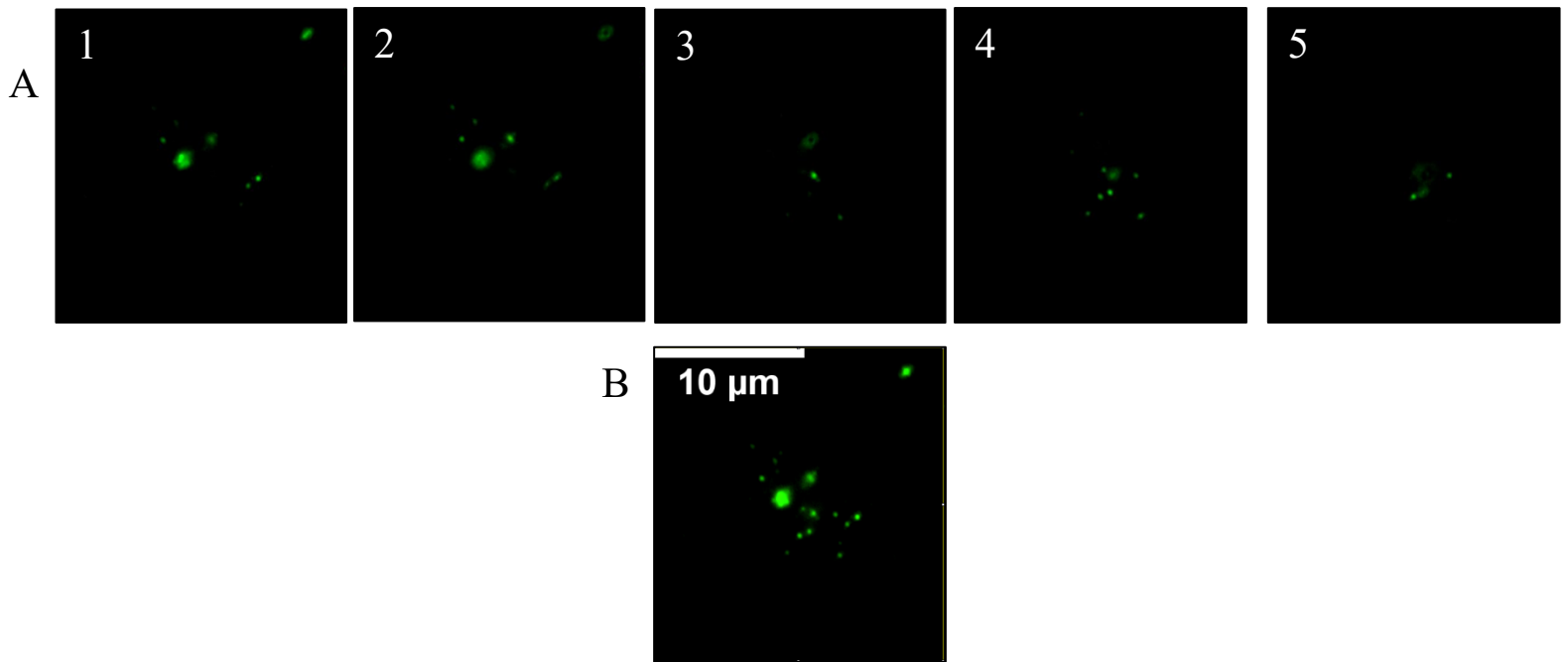


Figure 9 L929 nucleus stained with anti- γ H2AX (Ser139) (Merck Millipore, 05-636), anti-mouse secondary antibody Alexafluor488 (Thermofisher scientific, A21200).

A) Images from 1 to 5 are all images of the same nucleus stained with anti- γ H2AX taken at different planes. B) Merged image of images 1 to 5 showing all γ -H2AX foci in the same image.

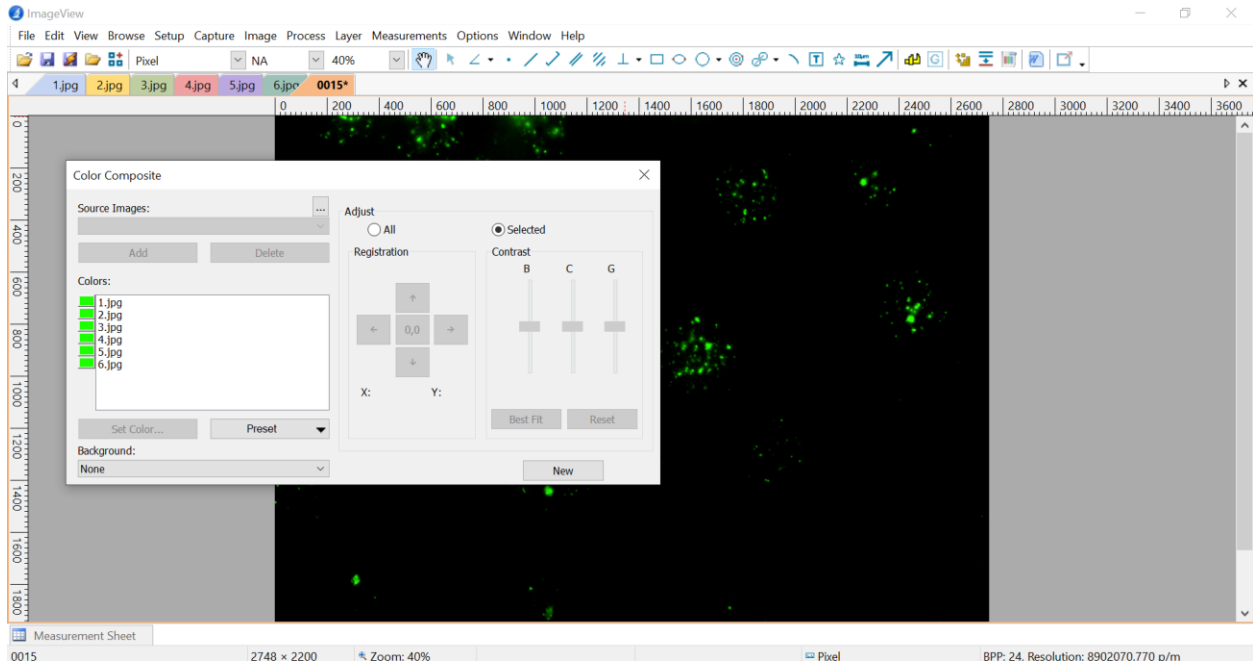


Figure 10 Screen shot showing the use of color composite tool on Imageview software to collate all γ -H2AX foci images into one.

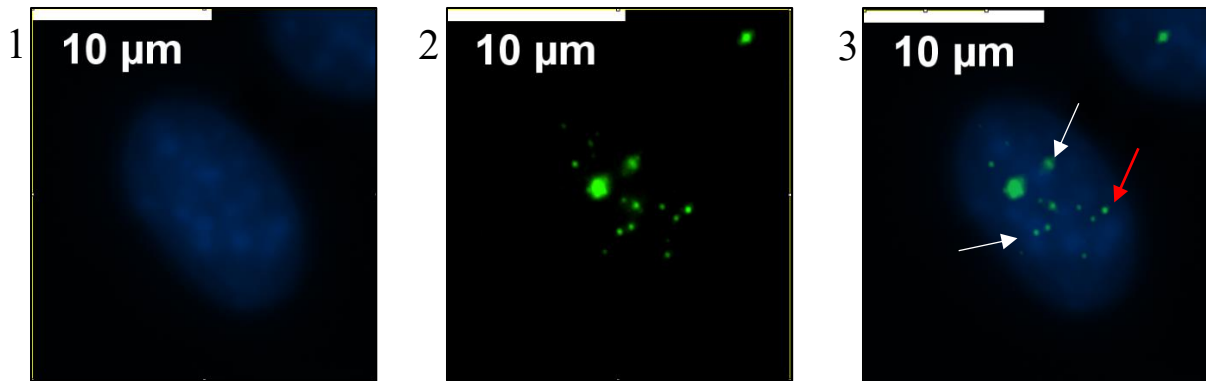


Figure 11 Merged images of L929 nucleus.

- 1) Overlay of all DAPI images. 2) Overlay of all γ -H2AX foci images. 3) Overlay of both collated DAPI images and γ -H2AX foci images to facilitate the scoring of γ -H2AX foci remaining in correlation with heterochromatin. (White arrows indicate foci associated with heterochromatin; red arrow indicates foci associated with euchromatin).

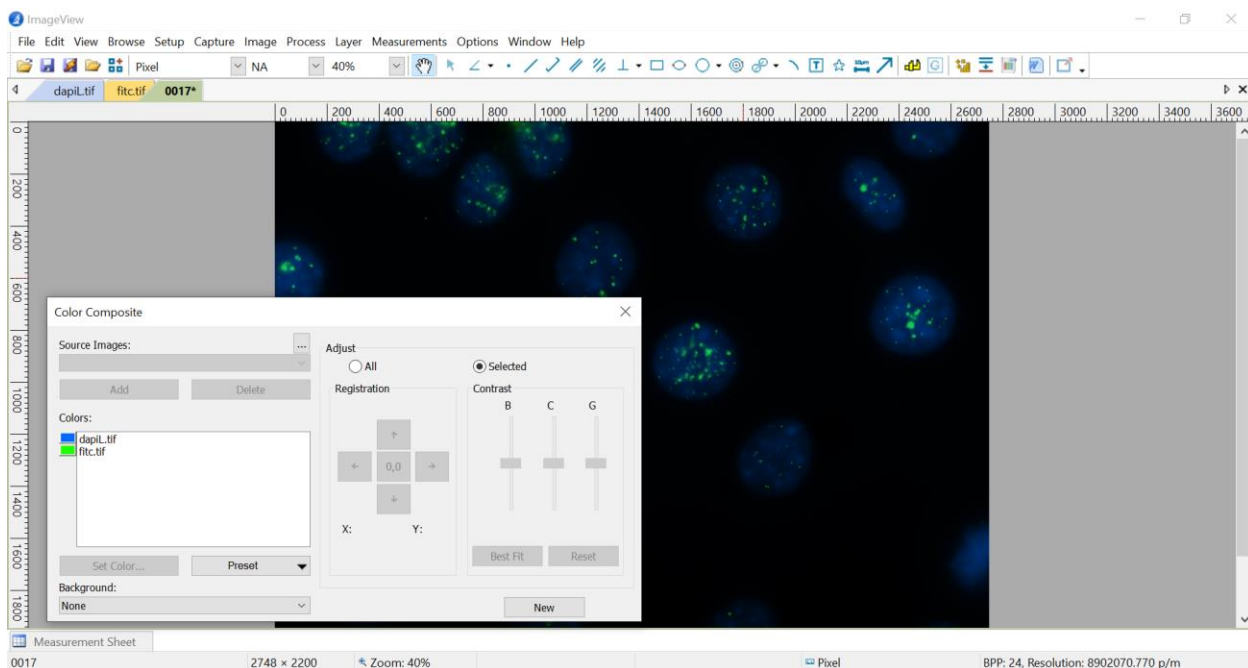


Figure 12 Screen shot showing the use of color composite tool on Imageview software to overlay the collated γ -H2AX foci image and the collated DAPI into one.

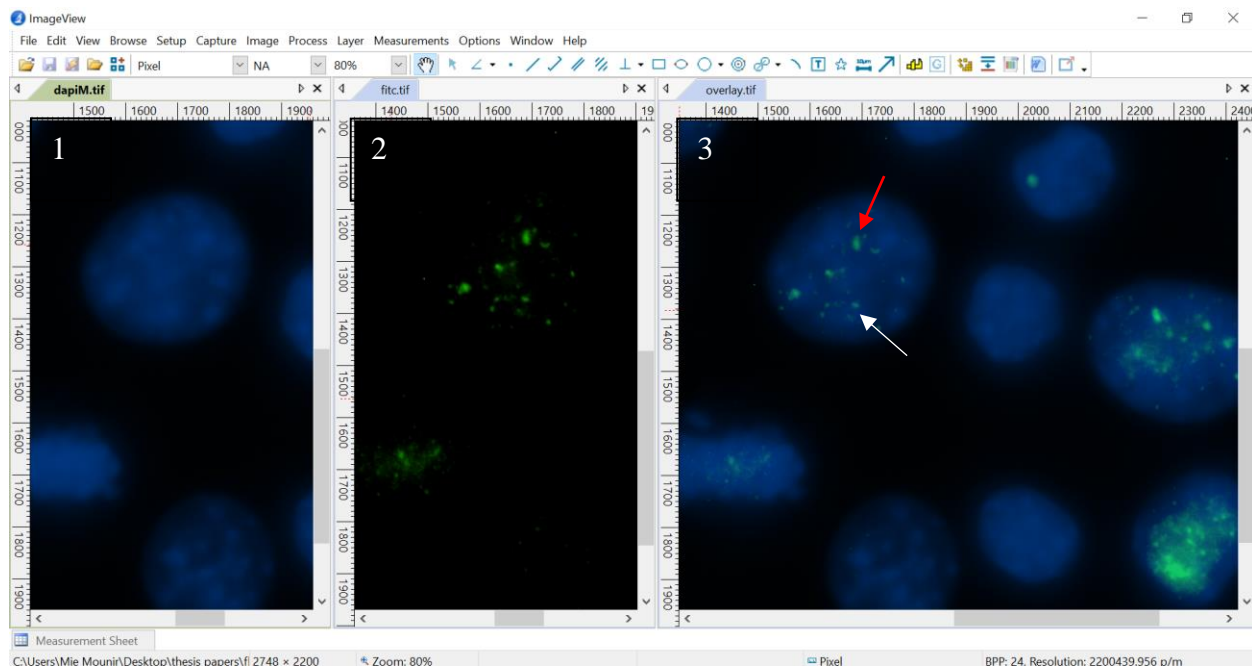


Figure 13 Counting of γ -H2AX foci from overlaid images of L929.

Total number of γ -H2AX foci is counted from 2. Heterochromatin associated foci is counted from 3. White arrow indicate foci associated with heterochromatin; red arrow indicates foci associated with euchromatin.

4.8 Assessment of DNA damage repair associated with heterochromatin after exposure to Neocarzinostatin and inhibition of Ataxia telangiectasia mutated.

L929 cells were seeded on coverslips at a density of (6×10^5) per well in a 6-well plate, then allowed to attach overnight. Afterwards $10 \mu\text{M}$ KU55933 (ATM inhibitor) (Goodarzi et al., 2008) was added to the attached cells for half an hour before adding the radiomimetic NCS. Then 50 ng/ml of NCS was added for 30 minutes. Then the coverslips are fixed at different time points of repair (0.5, 2, 5, 16, and 24 hours) (Goodarzi et al., 2008). A control coverslip was done with ATMi only and fixed after 24 hours of repair. The cells are stained with anti- γ H2AX (Ser139) (Merck Millipore, 05-636), anti-mouse secondary antibody Alexafluor488 (Thermofisher

scientific, A21200), and DAPI. Fixation and immunostaining were done as previously explained in 4.5 Immunostaining technique. Images were taken by Leica DM 2000 fluorescent microscope. Images were adjusted for scoring using ImageView and Fiji software as explained in (4.7 Assessment of DNA damage repair associated with heterochromatin after exposure to MNP.

4.9 Assessment of DNA damage repair associated with heterochromatin after exposure to MNP and inhibition of ATM.

L929 cells were seeded on coverslips at a density of (6×10^5) per well in a 6-well plate, then allowed to attach overnight. Then 10 μM KU55933 (ATM inhibitor) was added to the culture media for half an hour before adding the nanoparticles. Afterwards 5 $\mu\text{g/ml}$ of MNP were added for 24 hours. Subsequently, fresh media with ATMi is added; to remove the nanoparticles and to initiate the repair process. The cells are fixed at different time points of repair (0.5, 2, 5, 16, and 24 hours). A control coverslip was done with ATMi only and fixed after 24 hours of fresh media. The cells are stained with anti- γH2AX (Ser139) (Merck Millipore, 05-636), anti-mouse secondary antibody Alexafluor488 (Thermofisher scientific, A21200), and DAPI. Immunostaining and fixation were done as previously explained in 4.5 Immunostaining technique. Images were taken by Leica DM 2000 fluorescent microscope using the oil immersion lens (100x). Images were adjusted for scoring using ImageView and Fiji software as explained in (4.7 Assessment of DNA damage repair associated with heterochromatin after exposure to MNP.

4.10 Alkaline comet assay (Single cell gel electrophoresis)

L929 cell line was used in the alkaline comet assay. Cells were treated with increasing concentrations of MNPs (0.1, 1, 5, 10, 20 μ g/mL) MNPs for 24 hours, and cells treated with 1 μ M doxorubicin were used as positive control. Untreated cells were used as a negative control. A suspension of 10^5 treated cells were mixed with 200 μ L 1% low melting point agarose (LMA). Cells mixed with LMA were layered on standard agarose (0.8%) coated frosted slides. The slides were left to solidify, and then were submerged in alkaline lysis buffer pH 10 (2.5 M NaCl, 100 mM disodium EDTA dihydrate, 10 mM tris (pH 10), 10% DMSO, 1% triton) (Collins, 2004; Gomaa et al., 2013) overnight at 4°C. Before running the electrophoresis, the slides were equilibrated in cold electrophoresis buffer (pH 13) 1mM disodium EDTA dihydrate, 300 mM NaOH at 4 °C for 60 minutes. Afterwards, electrophoresis was done for 30 minutes 25 V/300mA at 4°C in cleaver scientific comet assay tank CSL-COM20. Then, the slides were neutralized with neutralization buffer 0.4 M tris pH 7.5. Subsequently stained with DAPI 5 μ g/ml. The slides were examined under the Leica DM 2000 fluorescent microscope. The images were analyzed using cometscore free software (Figure 14).

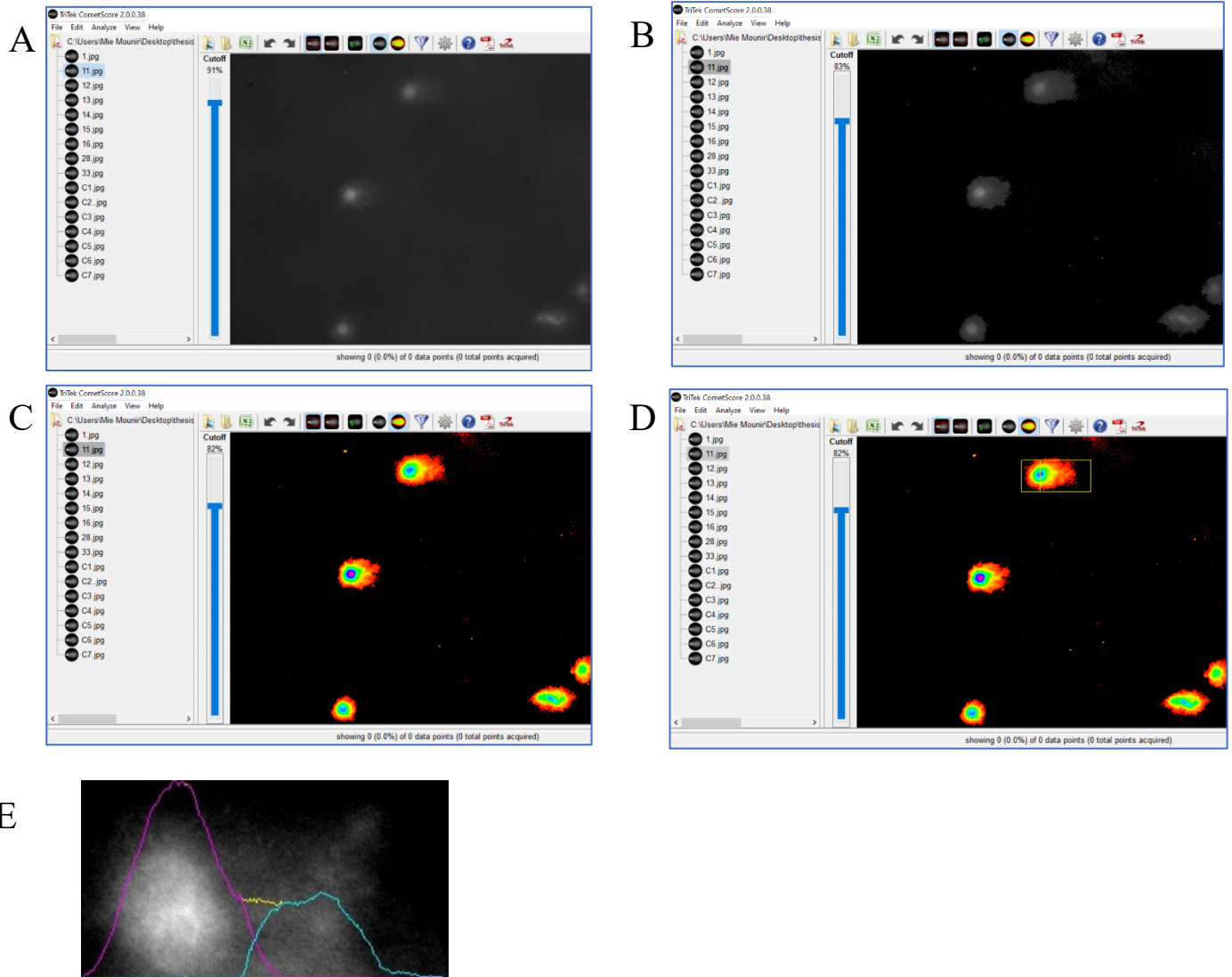


Figure 14 Image analysis on Cometscore software.

A-D adjusting cutoff and appointing comet heads for comet analysis to obtain different comet parameters. E) Purple curve represents the comet head diameter, head area, and comet length. Blue curve represents the tail area and tail length.

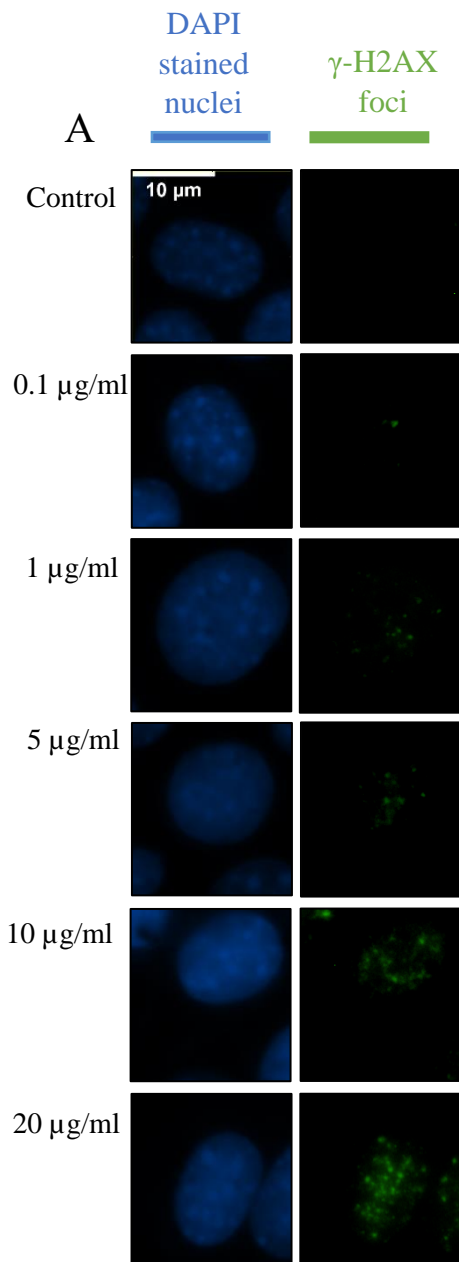
4.11 Statistical Analysis.

Triplicates of each experiment were done, and the mean values were calculated. Student's t-test was used to assess the significance of difference between the mean values of different conditions, and the p-value was set to be less than 0.05. The significant difference between different time points was done using ANOVA followed by Tukey multiple comparison test, the p-value was set to be less than 0.05.

5. Results.

5.1 Magnetite nanoparticles DNA double strand breaks dose response in L929.

Double strand breaks were assessed by counting γ -H2AX foci in L929 cell line after being subjected to increasing concentrations of MNPs for 24 hours. A proportional increase in the number of foci on increasing MNPs concentration was shown in L929 cell line (Figure 15).



B

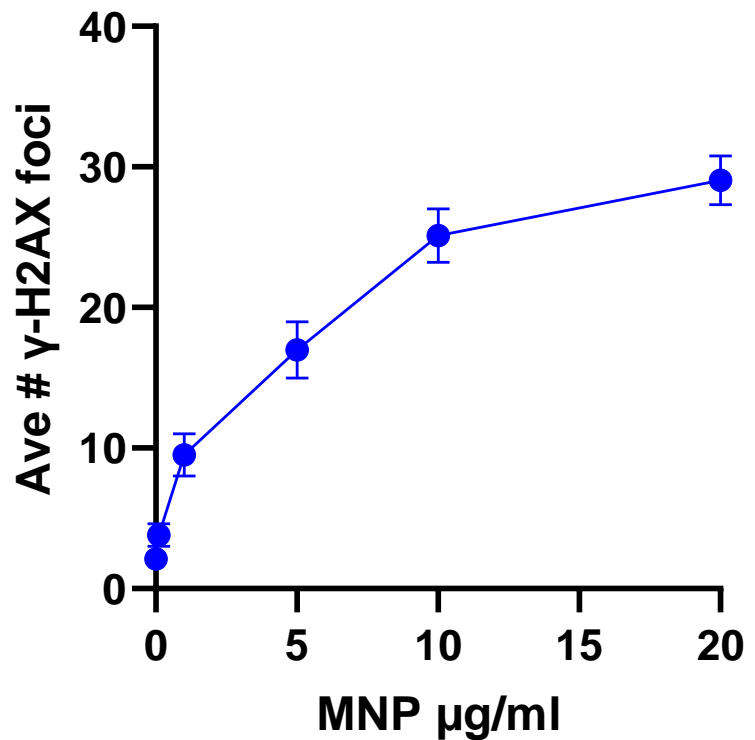


Figure 15 γ -H2AX foci in L929 cell line after exposure to increasing concentrations to MNPs.

(A) Images of nuclei of L929 cells fixed after 24 hours of exposure to increasing concentrations of magnetite nanoparticles (0.1, 1, 5, 10, and 20 $\mu\text{g/ml}$). (B) Graph showing the average γ -H2AX foci for each concentration.

5.2 Alkaline comet assay Single cell gel electrophoresis

Our preliminary data with comet assay also showed a dose proportionate response in the comets. The increasing percentage of DNA in the comet represents the increasing damaged fraction with the increasing dosage (Figure 16).

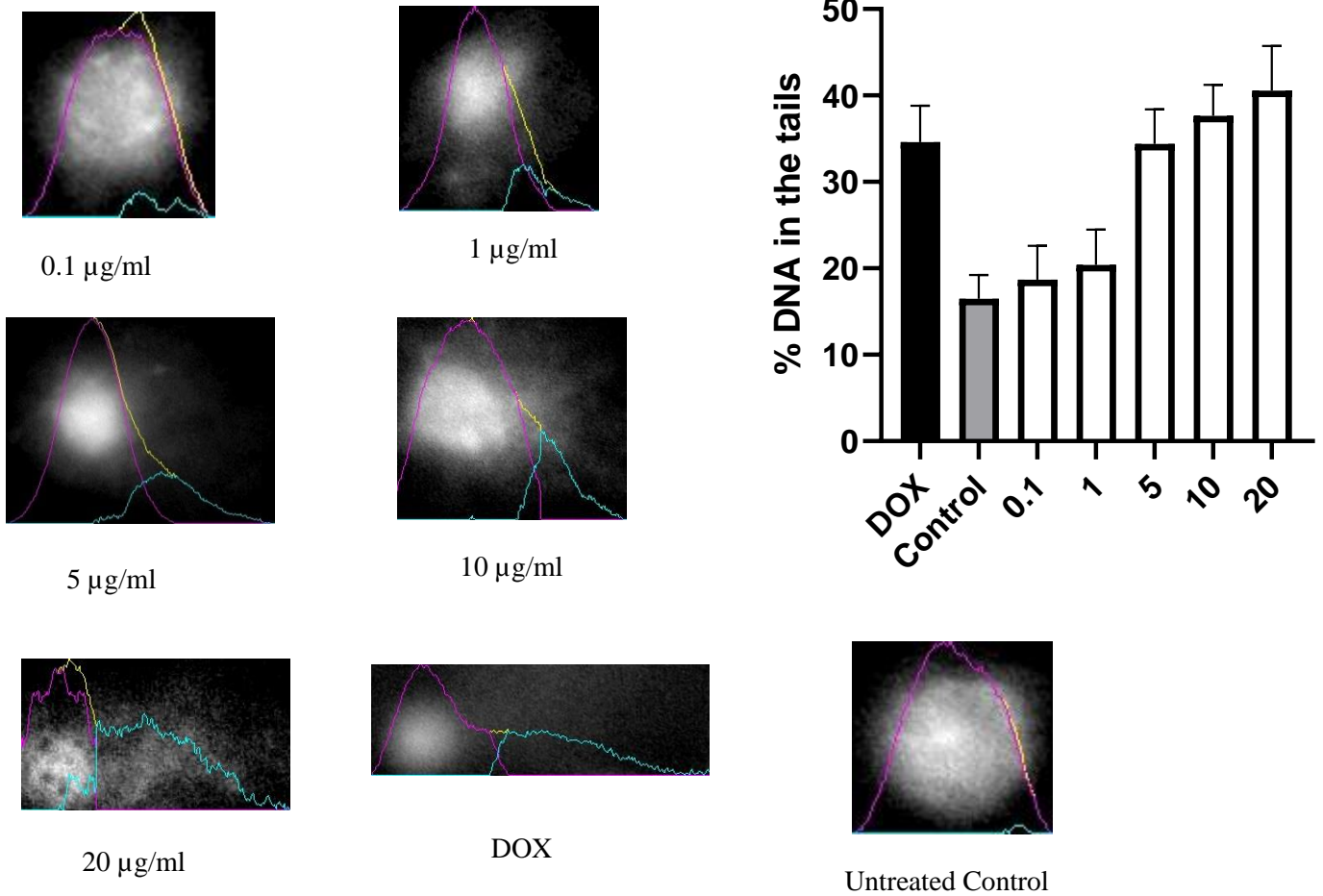


Figure 16 Percentage of DNA in comet tails in L929 cell line post exposure to MNPs.

A proportional response in the percentage of DNA in the tail, on increasing MNP concentration.

5.3 Heterochromatin Vs euchromatin repair kinetics after exposure to Magnetite nanoparticles.

Heterochromatin and euchromatin damage repair were assessed in the acrocentric murine cell line L929 after exposure to 5 $\mu\text{g/ml}$ MNPs. The cells were allowed to repair in fresh media, by 24 hours almost all $\gamma\text{-H2AX}$ foci were repaired (Figure 19). Only a small number of $\gamma\text{-H2AX}$ foci were remaining after 24 hours of repair. Those remaining foci were mostly found on the periphery of the densely stained heterochromatic regions. They constituted about 10.3 % of the total $\gamma\text{-H2AX}$ foci initially introduced. This percentage correlates with the percentage of DSBs that require ATM for repair (10-25%) (Riballo et al., 2004) (Figure 19). The $\gamma\text{-H2AX}$ foci associated with Euchromatin was found to repair 2 folds faster than heterochromatin associated foci (Figure 19). During monitoring the DSBs repair throughout the various time points, no changes in the heterochromatic chromocentres' structures were observed. There was a delay in the formation of the $\gamma\text{-H2AX}$ foci; they reached the maximum by 2 hours of changing into fresh media.

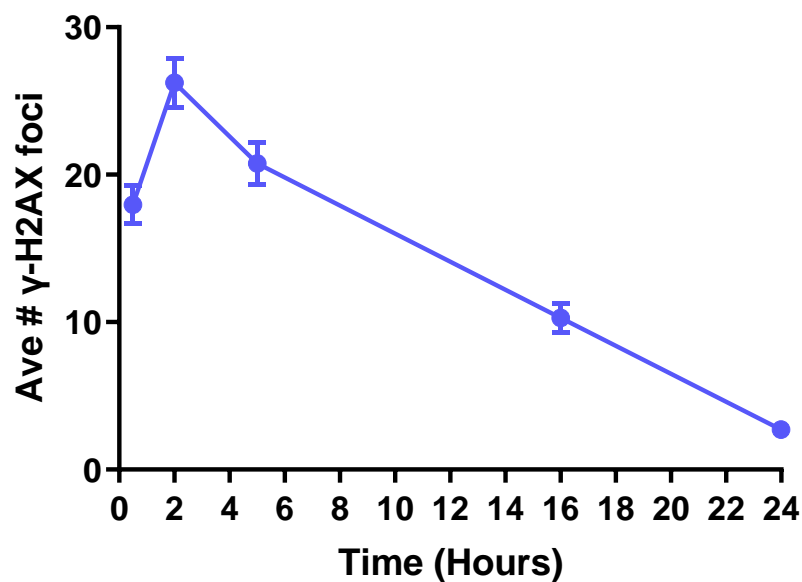


Figure 17 γ -H2AX foci resolution at 24 hours post MNP.

DNA damage repair kinetics were done by monitoring the resolution of γ -H2AX foci in L929 cell line, after exposure to 5 μ g/ml MNP for 24 hours. All results represent Mean \pm SEM of three experiments. 20 cells were counted per condition in each experiment (blind counting).

It is worth mentioning that the MNP persisted in a somewhat non-consistent manner around the nuclei of L929 after addition of fresh media (Figure 18). Consequently, these persisting nanoparticles influenced the scattering of the data to an extent.

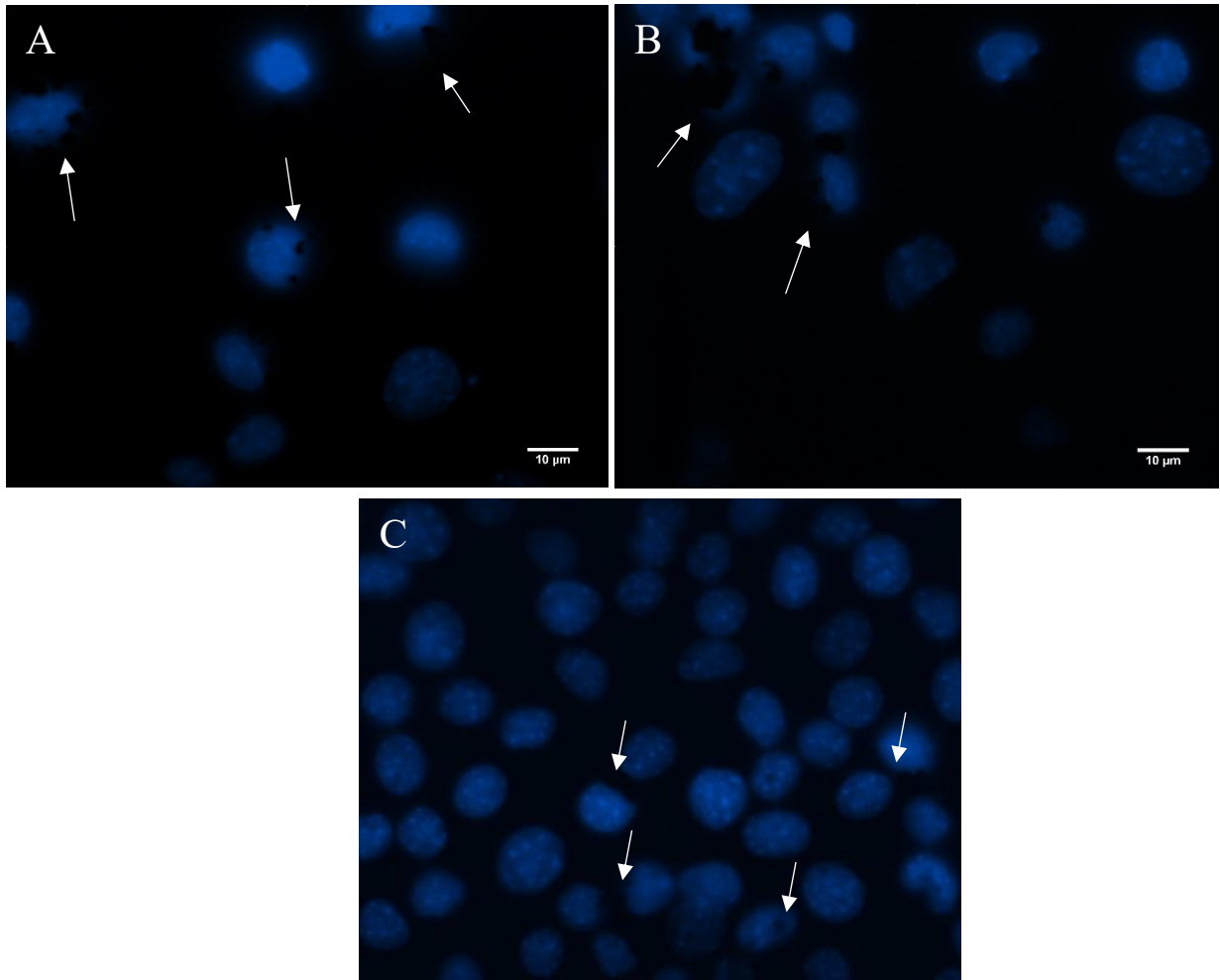


Figure 18 Persisting clumps of MNP around nuclei of L929.

(A) & (B) Images taken after 5 hours of repair in fresh media showing persisting clumps of magnetite nanoparticles around the nuclei of L929 cells. (C) Minute amounts of MNPs persisting at 16 hours of repair in fresh media.

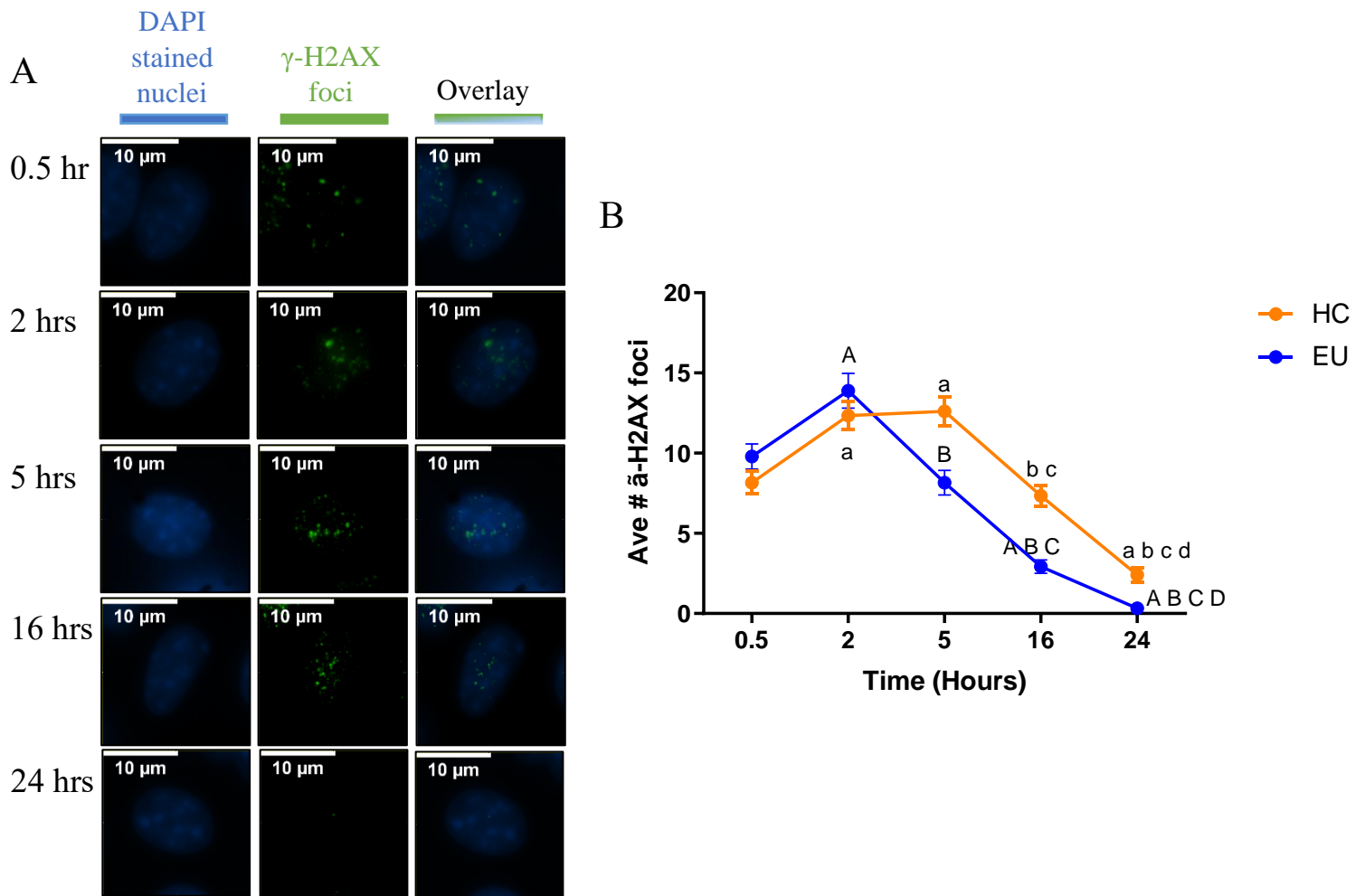


Figure 19 Heterochromatin and Euchromatin repair kinetics in L929 cell line.

Heterochromatin and Euchromatin repair in L929 cell line after exposure to 5 μ g/ml MNP for 24 hours and allowed to repair in fresh media for 24 hours. (A) Images of one cell for each time point of repair (0.5, 2, 5, 16, and 24 hours) showing the localization of DNA DSBs in heterochromatin and euchromatin. Each row of images represents one time point. The first image in each row is the DAPI stained nuclei, the second shows γ -H2AX foci, and the last is the overlay of both the DAPI and γ -H2AX foci images. At 24 hours almost all foci were repaired, and any remaining foci were at the periphery of high intensity heterochromatin areas. (B) Graph showing the percentage of heterochromatin and euchromatin associated foci at each time point. a or b or c or d: significantly different from 0.5, 2, 5, or 16 min respectively in HC γ -H2AX foci and at $P < 0.05$ using ANOVA

followed by Tukey multiple comparison test. A or B or C or D: significantly different from 0.5, 2, 5, or 16 min respectively in EC γ -H2AX foci and at $P < 0.05$ using ANOVA followed by Tukey multiple comparison test

The slowly repairing foci associated with heterochromatin captured at 8 hours of repair, appeared at the outlines of the densely stained areas of heterochromatin. Nevertheless, the γ -H2AX foci rarely appeared to fall within the chromocentres. Demonstrating the hinderance of the extension of γ -H2AX signal at 8 hours (Figure 20).

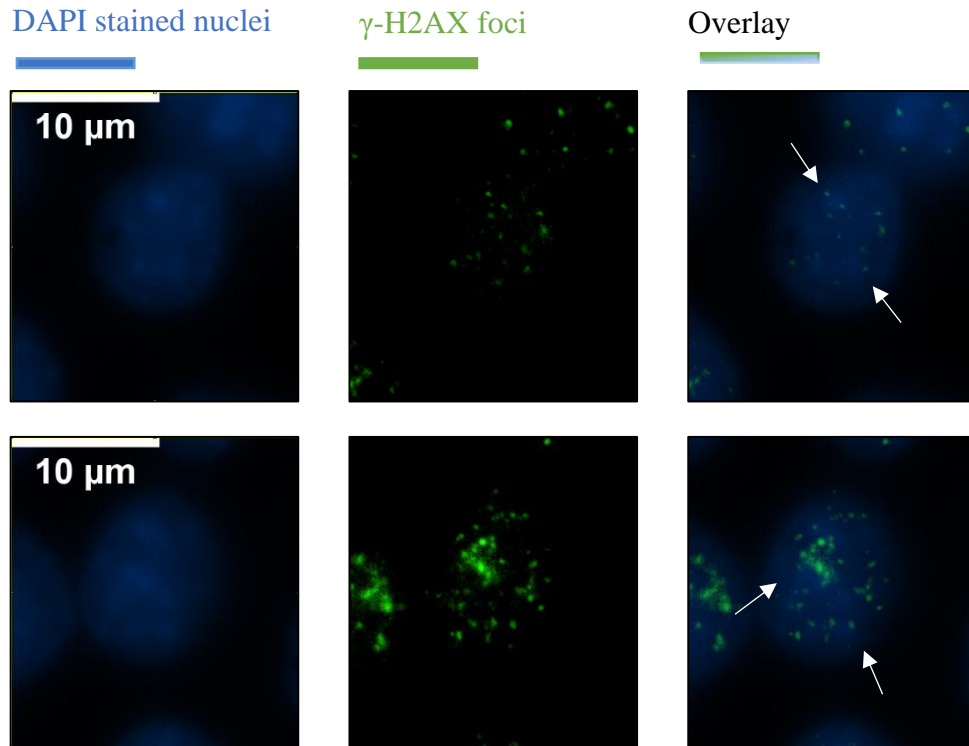


Figure 20 γ -H2AX foci localizing around high intensity DAPI stained regions of heterochromatin.

After 8 hours of repair persisting γ -H2AX foci mostly localized around high intensity DAPI stained regions of heterochromatin. These foci repaired by 24 hours. First image in each row is the DAPI stained nuclei, the second is γ -H2AX foci, and the third is the overlay of both previous.

5.4 Ataxia telangiectasia Mutated inhibition and Heterochromatin repair post Magnetite Nanoparticles.

ATM inhibited L929 cells (inhibited with 10 μ M KU55933), were exposed to 5 μ g/ml MNPs, and allowed to repair for 24 hours. On assessment of the γ -H2AX foci repair at each time point, we found that there was a significant increase in the number of foci introduced initially after inhibition

of ATM, in comparison with L929 cells treated only with MNP (Figure 21). At 24 hours significantly more γ -H2AX foci persisted in the ATM inhibited L929, and were associated at the periphery of heterochromatic regions (Figure 22). The percentage of heterochromatin associated foci by 16 hours increased by 22.7 % on inhibition of ATM. Inhibition of ATM had no significant effect on the repair of DSBs associated with euchromatin. There was comparable repair kinetics for the repair of the γ -H2AX foci post NCS/ATMi and MNP/ATMi treated L929 cells (Figure 22).

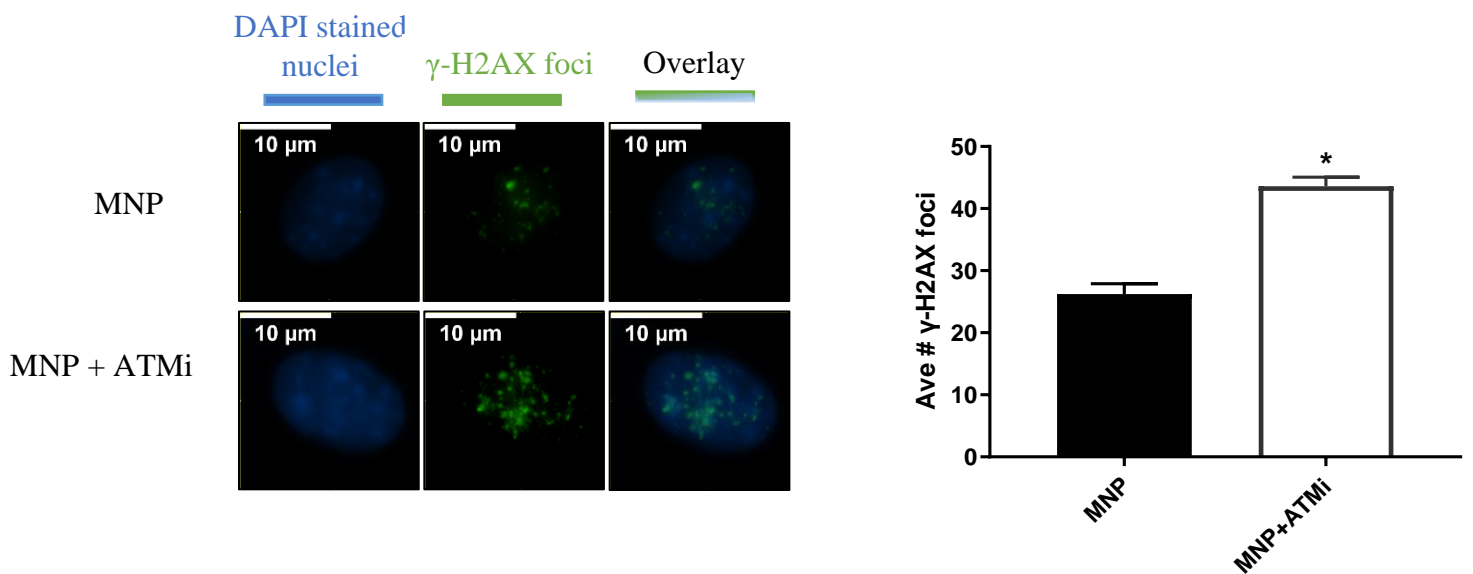


Figure 21 Initial γ -H2AX foci formed at 2 hours in MNP treated vs MNP/ATMi treated L929 cells.

A significant increase in the foci generated in MNP/ATMi treated L929 was found in comparison with MNP only treated L929. Student's T-test was used to show significance of the difference between means. Results generated from triplicates of each experiment.

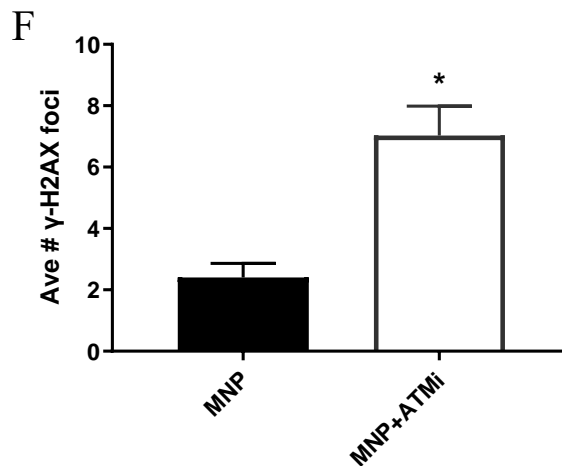
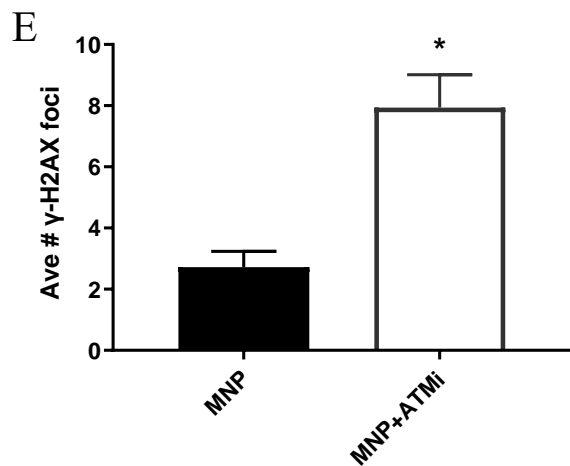
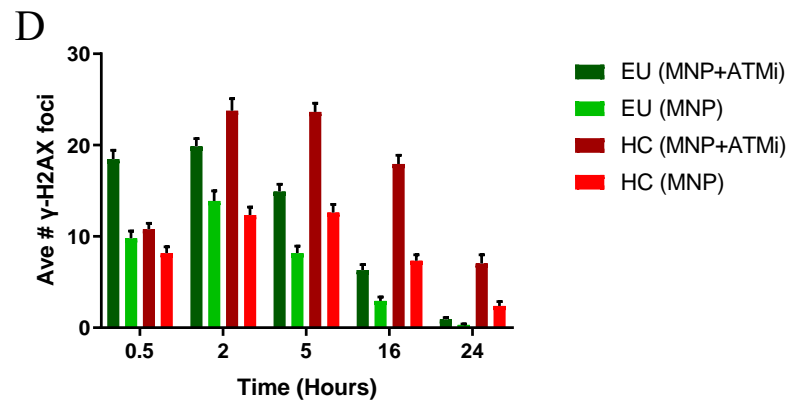
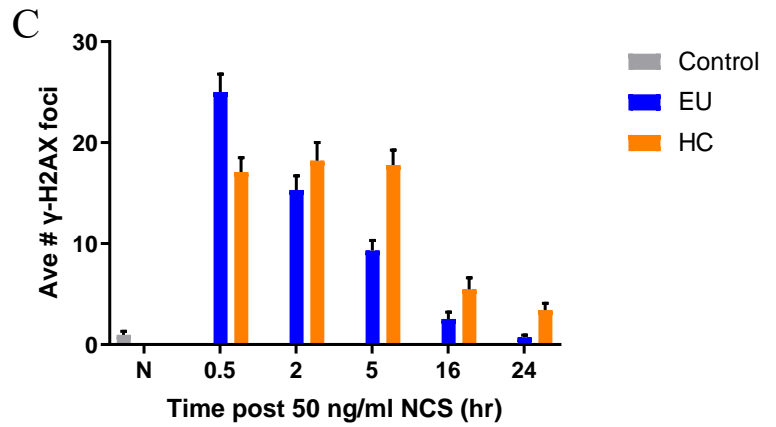
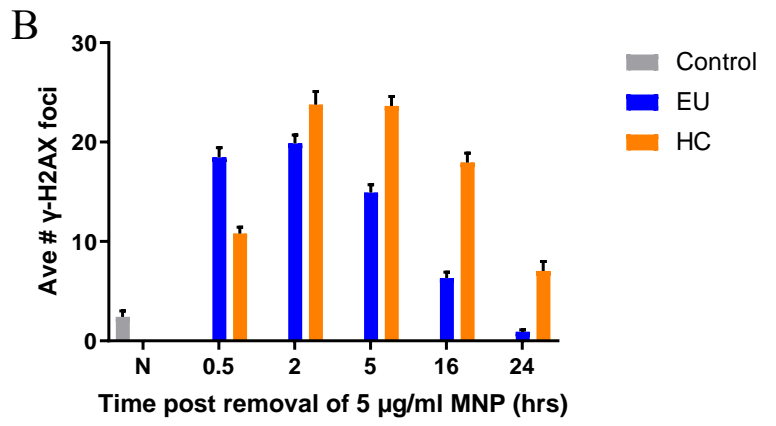
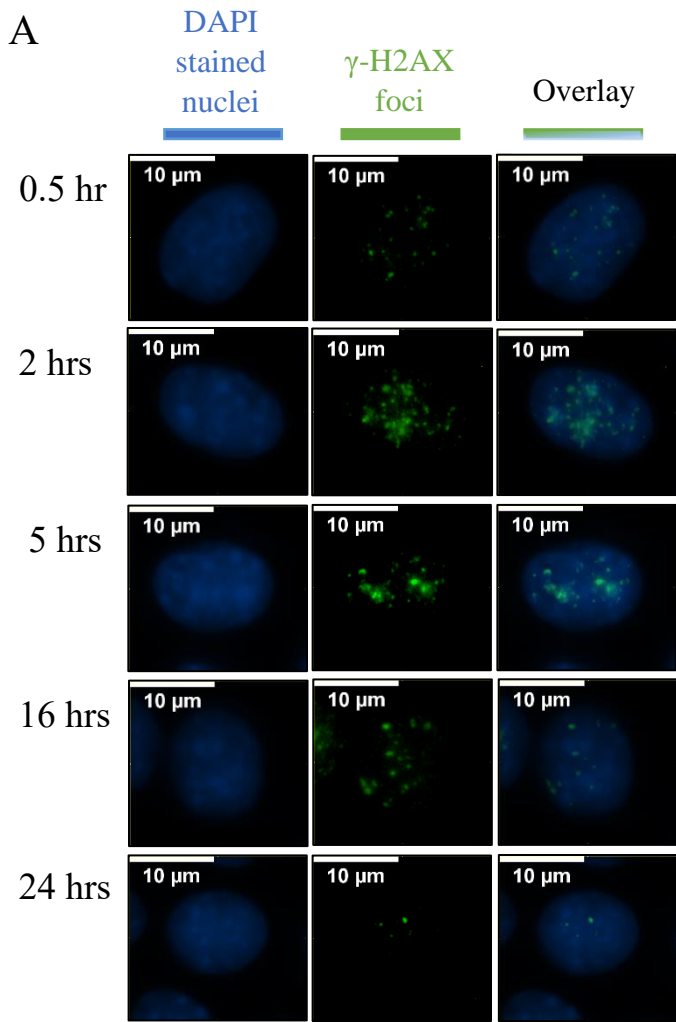


Figure 22 Heterochromatin vs euchromatin repair kinetics post MNP in L929 ATM inhibited cells.

A) Heterochromatin and Euchromatin repair in L929 cell line after exposure to 10 μ M ATMi (KU55933) and 5 μ g/ml MNP for 24 hours and allowed to repair in fresh media for 24 hours. (A) Images of one cell for each time point of repair (0.5, 2, 5, 16, and 24 hours) showing the localization of DNA DSBs in heterochromatin and euchromatin. Each row of images represents one time point. The first image in each row is the DAPI stained nuclei, the second shows γ -H2AX foci, and the last is the overlay of both the DAPI and γ -H2AX foci images. At 24 hours γ -H2AX foci persisted at the periphery of high intensity DAPI stained heterochromatin areas. B) Data collected from (A) was used to estimate the remaining foci around HC and EU at each time point. C) Resolution kinetics of γ -H2AX foci in L929 cells treated with 10 μ M ATMi (KU55933) and 50 ng/ml NCS (Images not shown). D) Repair kinetics of average γ -H2AX foci in HC and EU in ATM inhibited and non-inhibited post MNP. E) Significant difference between total number of foci at 24 hours between MNP treated cells and ATM inhibited cells treated with MNP (***P-value <0.001). F) Significant difference between HC associated foci in MNP treated cells vs MNP treated, ATM inhibited cells (***P-value<0.001). Significant difference between means of the experiment was assessed by Student's T-test. All results represent Mean \pm SEM of three experiments.

6. Discussion.

In this work, we reveal the genotoxicity of MNPs and the mechanisms required in the repair of DSBs formed in the higher chromatin structures. An important requirement for efficient repair of DSBs in heterochromatin is the accessibility of the DNA machinery to the damaged sites (White et al., 2012). It was rather imperative to study how the heterochromatin is rendered more relaxed and accessible for DNA repair after exposure to MNPs.

In our study, we used γ -H2AX foci analysis to detect DNA damage and monitor DNA repair, as it has been proven to be a sensitive and a reliable method. In contrast with pulsed field gel electrophoresis (PFGE) that requires high doses, which limits the significance of the findings (Riballo et al., 2004). We used G1 contact inhibited L929 cells to avoid complications and chromatin changes that happens during replication. Goodarzi et al., 2009 reported that at G1 the heterochromatin factors Kap-1 and H3K9me3 were highly enriched in densely DAPI stained regions of heterochromatin and depleted for euchromatin marker H3K9ac. On the contrary at G2 the heterochromatin markers were more diffuse and not exclusive to the chromocentres. At late G2 there was pan nuclear distribution of KAP-1 to allow chromosomal hypercondensation (Goodarzi et al., 2009). Therefore, G1 cells were more desirable to use to monitor the DSBs in heterochromatin, as the heterochromatin markers are unperturbed and restricted to the chromocentres.

On subjecting L929 murine cell line to increasing concentrations of MNP, a proportionate formation of γ -H2AX foci occurred. Representing the increasing formation of DSBs with the increasing dose, due to the generation of ROS as previously reported (Kawanishi et al., 2013; Sonmez et al., 2016; Valdiglesias et al., 2015).

We presume that the initial delay detected in the formation of γ -H2AX foci in the repair kinetics, marks the shift from the initial activation of ATM by oxidative stress into the activation of ATM by DSBs and the MRN complex (Blackford & Jackson, 2017; Guo et al., 2010). The activation of ATM by ROS produces the active cross-linked disulphide dimer that does not phosphorylate H2AX (Guo et al., 2010). However, the initially H2AX phosphorylation occurs to an extent and is not completely inhibited, as it is redundantly phosphorylated by DNA-PKcs and ATR (Pilch et al., 2003). Therefore, when the shift happened at 2 hours of repair; the activation of ATM into the active monomer by MRN complex at the sites of DSBs; more γ -H2AX foci appeared.

It is worth mentioning that MNPs are different from IR and radiomimetic drugs in their genotoxic effect, as we observed marked persistence of MNPs in the nuclei even after removing the nanoparticle and incubating the cells with fresh media. Consequently, we presume that MNPs persistence cause a dynamic state of damage and repair, that caused scattering in the number of foci to an extent. By 24 hours almost none or very minute amounts of nanoparticles were present in the nuclei.

Throughout the observation of the repair of DSBs post exposure to MNP, the DSBs associated with heterochromatin were almost always found on the periphery of the chromocentres, and rarely found within. Which attests that heterochromatin serves as a physical barrier for the extension of DNA repair signal and retards the repair machinery. For the first time to our knowledge, we detected a 2-fold delay in the repair of the DSBs associated with heterochromatin in comparison with euchromatin in the γ -H2AX foci generated after MNPs exposure.

In our experiments with MNPs we demonstrated the requirement of ATM in the repair of the DSBs associated with heterochromatin, as the repair of the γ -H2AX foci in heterochromatin was significantly perturbed on inhibition of ATM, supported by the findings of Goodarzi et al., 2008

on the role of ATM in repair of DSBs in heterochromatin post IR. ATM controls the relaxation of the tightly compacted heterochromatic structures through phosphorylation of the heterochromatic protein Kap-1 causing a transient relaxation in the nucleosome to allow extension of the DNA repair signal (Blackford & Jackson, 2017; Goodarzi et al., 2008, 2009, 2010; Ziv et al., 2006). We also demonstrate that there was comparable repair defect in heterochromatin DSBs after inhibition of ATM post 5 μ g/ml MNP and 50 ng/ml NCS. Goodarzi et al., 2008 demonstrated that 50 ng/ml NCS heterochromatin repair kinetics was comparable to 2 Gy IR in ATM^{-/-} cells.

No changes in the chromocentres' structures were detected while monitoring the DSBs associated with heterochromatin post MNP, so it is highly unlikely that ATM dismantles the heterochromatin superstructure. Therefore, we presume that only a transient relaxation happens. Agreeing with the work previously done by Goodarzi et al., 2008, 2009, 2010 and White et al., 2012.

The significant persistence of the γ -H2AX foci around the heterochromatin regions on inhibition of ATM demonstrates the predominant reliance on ATM for the relaxation of nucleosomes, and that other PIKKs; ATR and DNA-PKcs are either not involved, or have minimal contribution in the repair of the heterochromatin DSBs post exposure to MNP. Agreeing with the findings of Goodarzi et al., 2009 on inhibition of ATR there was no significant reduction of phosphorylation of Kap-1 post IR.

On inhibition of ATM the overall number of γ -H2AX foci generated initially increased as expected, as ATM is reported to regulate the oxidative stress as previously reported (Guo et al., 2010) resulting in more DNA damage foci overall. However, by 24 hours all the euchromatin foci were resolved and there was no significant difference between ATMi treated and non-treated. On the contrary there was a significant difference between the number of foci remaining at the borders of the heterochromatin between ATMi treated and non-treated, highlighting the importance of

ATM in reducing the oxidative stress and resolution of DNA damage associated with heterochromatin post exposure to MNP.

The underlying mechanisms of the relaxation of heterochromatin post exposure to MNP is still to be determined. However, strong evidence points to the similarity in the mechanism of ATM mediated repair of heterochromatin post IR and MNP. To begin the relaxation of heterochromatin post IR, ATM phosphorylates KAP-1 at S 824. The mutation S824A conferred an ATM defect in presence or absence in ATM, while the mutation S824D (constitutive phosphorylation of S 824) alleviated the need for ATM, indicating the necessity of S 824 phosphorylation. Knock down of any of those heterochromatinization factors KAP-1, HDAC1/2, Suv39H1/2 and HP 1 alleviated the need for ATM (Goodarzi et al., 2008, 2009, 2010). KAP-1 phosphorylation is transient and highly dose dependent. It does not disrupt the higher heterochromatin structure (Goodarzi et al., 2009). Goodarzi et al., 2010 stated that there was no difference in the interaction between pKAP-1 and other heterochromatic factors as HP-1, or HDAC 1/2 on introduction of IR. There was only a change in the nucleosomal compaction and rendering them more prone to nuclease digestion in vitro (Ziv et al., 2006). Also, the phosphorylation of KAP-1 prevented its auto-SUMOylation which in turn affected its binding with the heterochromatin remodeller CHD3/Mi-2 α and SETDB1 histone methyltransferase (Ivanov et al., 2007; Schultz et al., 2002). The repair kinetics of heterochromatin remained significantly slower than euchromatin, even after knockdown of KAP-1 or expression of a constitutively phosphorylated version S824D. which shows that the phosphorylation of KAP-1 doesn't result in Euchromatinization, but only cause a relaxation in the nucleosome bonds.

Finally, we would like to emphasize the role of ATM in the repair of the heterochromatin associated DSBs induced by MNPs, and to highlight MNPs sensitivity would increase in Ataxia

telangiectasia patients that lack functional ATM. We propose that A-T patients lacking ATM would lack the proper machinery for relaxation of heterochromatin to repair DSBs associated with higher chromatin structures. Therefore, after being exposed to MNPs present abundantly in particulate matter air pollution in large cities (Calderón-Garcidueñas et al., 2019; González-Maciel et al., 2017; Grobety et al., 2010; Maher et al., 2016), they would accumulate DNA damage in heterochromatin. Although heterochromatin is mainly composed of repetitive stretches of satellite DNA (Craig, 2005), accumulating DNA damage compromises telomeres and the silenced genes near the pericentromeric regions that are silenced by the effect of spreading nature of heterochromatin factors.

7. Conclusion.

DNA repair of MNPs induced DSBs in heterochromatin requires ATM for relaxation of the compacted structure and allowing the extension the repair signal. No visible alteration in the structure of chromocentres happened during the repair of HC DSBs. ATR and DNA-PKcs did not compensate the repair defect in heterochromatin on inhibition of ATM. Not only ATM controls ROS levels in the cell, controls cell cycle checkpoints, contributes profoundly to DNA repair mechanism but also, it contributes to the relaxation of heterochromatin post MNP exposure.

8. Prospects.

For further inspection of role of ATM to relax heterochromatin post exposure to MNPs, we want to inspect if KAP-1 is one of the downstream targets of ATM. Through Knocking down of KAP-1, monitoring if the repair defect in presence and absence of ATM. Also, we would want to test if the absence of other heterochromatin markers (HP 1 and HDAC1/2) that interacts with KAP-1, would alleviate the need for ATM. Also, we want to confirm that ATR and DNA-PKcs have no/minute effect on heterochromatin relaxation post MNP utilizing DNA-PKcs^{-/-} and ATR^{-/-} cells. We would also test the invitro availability of Kap-1 in chromatin fractions on nuclease digestion post MNP with or without the presence of ATM.

9. References.

- Ahringer, J. (2000). NuRD and SIN3: Histone deacetylase complexes in development. *Trends in Genetics*, 16(8), 351–356. [https://doi.org/10.1016/S0168-9525\(00\)02066-7](https://doi.org/10.1016/S0168-9525(00)02066-7)
- Ayyanathan, K., Lechner, M. S., Bell, P., Maul, G. G., Schultz, D. C., Yamada, Y., Tanaka, K., Torigoe, K., & Rauscher, F. J. (2003). Regulated recruitment of HP1 to a euchromatic gene induces mitotically heritable, epigenetic gene silencing: A mammalian cell culture model of gene variegation. *Genes & Development*, 17(15), 1855–1869. <https://doi.org/10.1101/gad.1102803>
- Babbs, C. F., Cregor, M. D., Turek, J. J., & Badylak, S. F. (1991). Endothelial superoxide production in buffer perfused rat lungs, demonstrated by a new histochemical technique. *Laboratory Investigation; a Journal of Technical Methods and Pathology*, 65(4), 484–496.
- Babior, B. M., & Woodman, R. C. (1990). Chronic granulomatous disease. *Seminars in Hematology*, 27(3), 247–259.
- Bakkenist, C. J., & Kastan, M. B. (2003). DNA damage activates ATM through intermolecular autophosphorylation and dimer dissociation. *Nature*, 421(6922), 499–506. <https://doi.org/10.1038/nature01368>
- Bannister, A. J., Gottlieb, T. M., Kouzarides, T., & Jackson, S. P. (1993). C-Jun is phosphorylated by the DNA-dependent protein kinase *in vitro*; definition of the minimal kinase recognition motif. *Nucleic Acids Research*, 21(5), 1289–1295. <https://doi.org/10.1093/nar/21.5.1289>

- Barzilai, A. (2002). ATM deficiency and oxidative stress: A new dimension of defective response to DNA damage. *DNA Repair*, 1(1), 3–25. [https://doi.org/10.1016/S1568-7864\(01\)00007-6](https://doi.org/10.1016/S1568-7864(01)00007-6)
- Blackford, A. N., & Jackson, S. P. (2017). ATM, ATR, and DNA-PK: The Trinity at the Heart of the DNA Damage Response. *Molecular Cell*, 66(6), 801–817. <https://doi.org/10.1016/j.molcel.2017.05.015>
- Brockdorff, N. (2002). X-chromosome inactivation: Closing in on proteins that bind Xist RNA. *Trends in Genetics*, 18(7), 352–358. [https://doi.org/10.1016/S0168-9525\(02\)02717-8](https://doi.org/10.1016/S0168-9525(02)02717-8)
- Calderón-Garcidueñas, L., González-Maciel, A., Mukherjee, P. S., Reynoso-Robles, R., Pérez-Guillé, B., Gayosso-Chávez, C., Torres-Jardón, R., Cross, J. V., Ahmed, I. A. M., Karloukovski, V. V., & Maher, B. A. (2019). Combustion- and friction-derived magnetic air pollution nanoparticles in human hearts. *Environmental Research*, 176, 108567. <https://doi.org/10.1016/j.envres.2019.108567>
- Calderón-Garcidueñas, L., Reynoso-Robles, R., Pérez-Guillé, B., Mukherjee, P. S., & González-Maciel, A. (2017). Combustion-derived nanoparticles, the neuroenteric system, cervical vagus, hyperphosphorylated alpha synuclein and tau in young Mexico City residents. *Environmental Research*, 159, 186–201. <https://doi.org/10.1016/j.envres.2017.08.008>
- Calderón-Garcidueñas, L., Reynoso-Robles, R., Vargas-Martínez, J., Gómez-Maqueo-Chew, A., Pérez-Guillé, B., Mukherjee, P. S., Torres-Jardón, R., Perry, G., & González-Maciel, A. (2016). Prefrontal white matter pathology in air pollution exposed Mexico City young urbanites and their potential impact on neurovascular unit dysfunction and the development of Alzheimer's disease. *Environmental Research*, 146, 404–417. <https://doi.org/10.1016/j.envres.2015.12.031>

- Cao, R., Wang, L., Wang, H., Xia, L., Erdjument-Bromage, H., Tempst, P., Jones, R. S., & Zhang, Y. (2002). Role of Histone H3 Lysine 27 Methylation in Polycomb-Group Silencing. *Science*, *298*(5595), 1039–1043. <https://doi.org/10.1126/science.1076997>
- Chen, Y. R., Lees-Miller, S. P., Tegtmeyer, P., & Anderson, C. W. (1991). The human DNA-activated protein kinase phosphorylates simian virus 40 T antigen at amino- and carboxy-terminal sites. *Journal of Virology*, *65*(10), 5131–5140. <https://doi.org/10.1128/JVI.65.10.5131-5140.1991>
- Collins, A. R. (2004). The comet assay for DNA damage and repair. *Molecular Biotechnology*, *26*(3), 249. <https://doi.org/10.1385/MB:26:3:249>
- Cosentino, C., Grieco, D., & Costanzo, V. (2011). ATM activates the pentose phosphate pathway promoting anti-oxidant defence and DNA repair: ATM activates the pentose phosphate pathway. *The EMBO Journal*, *30*(3), 546–555. <https://doi.org/10.1038/emboj.2010.330>
- Craig, J. M. (2005). Heterochromatin? many flavours, common themes. *BioEssays*, *27*(1), 17–28. <https://doi.org/10.1002/bies.20145>
- Crawford, T. O., Skolasky, R. L., Fernandez, R., Rosquist, K. J., & Lederman, H. M. (2006). Survival probability in ataxia telangiectasia. *Archives of Disease in Childhood*, *91*(7), 610–611. <https://doi.org/10.1136/adc.2006.094268>
- Crawford, Thomas O. (1998). Ataxia telangiectasia. *Seminars in Pediatric Neurology*, *5*(4), 287–294. [https://doi.org/10.1016/S1071-9091\(98\)80007-7](https://doi.org/10.1016/S1071-9091(98)80007-7)
- Czornak, K., Chughtai, S., & Chrzanowska, K. H. (2008). Mystery of DNA repair: The role of the MRN complex and ATM kinase in DNA damage repair. *Journal of Applied Genetics*, *49*(4), 383–396. <https://doi.org/10.1007/BF03195638>

- Dare, S. A. S., Barnes, S.-J., Beaudoin, G., Méric, J., Boutroy, E., & Potvin-Doucet, C. (2014). Trace elements in magnetite as petrogenetic indicators. *Mineralium Deposita*, *49*(7), 785–796. <https://doi.org/10.1007/s00126-014-0529-0>
- Donaldson, K., Stone, V., Tran, C. L., Kreyling, W., & Borm, P. J. A. (2004). Nanotoxicology. *Occupational and Environmental Medicine*, *61*(9), 727–728. <https://doi.org/10.1136/oem.2004.013243>
- Donaldson, Ken, & Tran, C. L. (2002). INFLAMMATION CAUSED BY PARTICLES AND FIBERS. *Inhalation Toxicology*, *14*(1), 5–27. <https://doi.org/10.1080/089583701753338613>
- Evans, J., Maccabee, M., Hatahet, Z., Courcelle, J., Bockrath, R., Ide, H., & Wallace, S. (1993). Thymine ring saturation and fragmentation products: Lesion bypass, misinsertion and implications for mutagenesis. *Mutation Research/Genetic Toxicology*, *299*(3), 147–156. [https://doi.org/10.1016/0165-1218\(93\)90092-R](https://doi.org/10.1016/0165-1218(93)90092-R)
- Foray, N. (2003). A subset of ATM- and ATR-dependent phosphorylation events requires the BRCA1 protein. *The EMBO Journal*, *22*(11), 2860–2871. <https://doi.org/10.1093/emboj/cdg274>
- Fournier, C., Goto, Y., Ballestar, E., Delaval, K., Hever, A. M., Esteller, M., & Feil, R. (2002). Allele-specific histone lysine methylation marks regulatory regions at imprinted mouse genes. *The EMBO Journal*, *21*(23), 6560–6570. <https://doi.org/10.1093/emboj/cdf655>
- Fridovich, I. (1989). Superoxide dismutases. An adaptation to a paramagnetic gas. *The Journal of Biological Chemistry*, *264*(14), 7761–7764.

- Gieré, R. (2016). Magnetite in the human body: Biogenic vs. anthropogenic. *Proceedings of the National Academy of Sciences*, *113*(43), 11986–11987.
<https://doi.org/10.1073/pnas.1613349113>
- Gomaa, I. O., Kader, M. H. A., Eldin, T. A. S., & Heikal, O. A. (2013). *Evaluation of in vitro mutagenicity and genotoxicity of magnetite nanoparticles*. 9.
- González-Maciél, A., Reynoso-Robles, R., Torres-Jardón, R., Mukherjee, P. S., & Calderón-Garcidueñas, L. (2017). Combustion-Derived Nanoparticles in Key Brain Target Cells and Organelles in Young Urbanites: Culprit Hidden in Plain Sight in Alzheimer's Disease Development. *Journal of Alzheimer's Disease*, *59*(1), 189–208.
<https://doi.org/10.3233/JAD-170012>
- Goodarzi, A. A., Jeggo, P., & Lobrich, M. (2010). The influence of heterochromatin on DNA double strand break repair: Getting the strong, silent type to relax. *DNA Repair*, *9*(12), 1273–1282. <https://doi.org/10.1016/j.dnarep.2010.09.013>
- Goodarzi, A. A., Noon, A. T., Deckbar, D., Ziv, Y., Shiloh, Y., Löbrich, M., & Jeggo, P. A. (2008). ATM Signaling Facilitates Repair of DNA Double-Strand Breaks Associated with Heterochromatin. *Molecular Cell*, *31*(2), 167–177.
<https://doi.org/10.1016/j.molcel.2008.05.017>
- Goodarzi, A. A., Noon, A. T., & Jeggo, P. A. (2009). The impact of heterochromatin on DSB repair. *Biochemical Society Transactions*, *37*(3), 569–576.
<https://doi.org/10.1042/BST0370569>
- Grobety, B., Giere, R., Dietze, V., & Stille, P. (2010). Airborne Particles in the Urban Environment. *Elements*, *6*(4), 229–234. <https://doi.org/10.2113/gselements.6.4.229>

- Guo, Z., Kozlov, S., Lavin, M. F., Person, M. D., & Paull, T. T. (2010). ATM activation by oxidative stress. *Science (New York, N.Y.)*, *330*(6003), 517–521.
<https://doi.org/10.1126/science.1192912>
- Hadjipanayis, C. G., Bonder, M. J., Balakrishnan, S., Wang, X., Mao, H., & Hadjipanayis, G. C. (2008). Metallic Iron Nanoparticles for MRI Contrast Enhancement and Local Hyperthermia. *Small*, *4*(11), 1925–1929. <https://doi.org/10.1002/sml.200800261>
- Huisinga, K. L., Brower-Toland, B., & Elgin, S. C. R. (2006). The contradictory definitions of heterochromatin: Transcription and silencing. *Chromosoma*, *115*(2), 110–122.
<https://doi.org/10.1007/s00412-006-0052-x>
- Ivanov, A. V., Peng, H., Yurchenko, V., Yap, K. L., Negorev, D. G., Schultz, D. C., Psulkowski, E., Fredericks, W. J., White, D. E., Maul, G. G., Sadofsky, M. J., Zhou, M.-M., & Rauscher, F. J. (2007). PHD Domain-Mediated E3 Ligase Activity Directs Intramolecular Sumoylation of an Adjacent Bromodomain Required for Gene Silencing. *Molecular Cell*, *28*(5), 823–837. <https://doi.org/10.1016/j.molcel.2007.11.012>
- Johansson, C., & Johansson, P.-Å. (2003). Particulate matter in the underground of Stockholm. *Atmospheric Environment*, *37*(1), 3–9. [https://doi.org/10.1016/S1352-2310\(02\)00833-6](https://doi.org/10.1016/S1352-2310(02)00833-6)
- Kawanishi, M., Ogo, S., Ikemoto, M., Totsuka, Y., Ishino, K., Wakabayashi, K., & Yagi, T. (2013). Genotoxicity and reactive oxygen species production induced by magnetite nanoparticles in mammalian cells. *The Journal of Toxicological Sciences*, *38*(3), 503–511. <https://doi.org/10.2131/jts.38.503>
- Kim, J.-A., Kruhlak, M., Dotiwala, F., Nussenzweig, A., & Haber, J. E. (2007). Heterochromatin is refractory to γ -H2AX modification in yeast and mammals. *Journal of Cell Biology*, *178*(2), 209–218. <https://doi.org/10.1083/jcb.200612031>

- Kim, S.-T., Lim, D.-S., Canman, C. E., & Kastan, M. B. (1999). Substrate Specificities and Identification of Putative Substrates of ATM Kinase Family Members. *Journal of Biological Chemistry*, 274(53), 37538–37543. <https://doi.org/10.1074/jbc.274.53.37538>
- Könczöl, M., Ebeling, S., Goldenberg, E., Treude, F., Gminski, R., Gieré, R., Grobéty, B., Rothen-Rutishauser, B., Merfort, I., & Mersch-Sundermann, V. (2011). Cytotoxicity and Genotoxicity of Size-Fractionated Iron Oxide (Magnetite) in A549 Human Lung Epithelial Cells: Role of ROS, JNK, and NF- κ B. *Chemical Research in Toxicology*, 24(9), 1460–1475. <https://doi.org/10.1021/tx200051s>
- Kourmouli, N., Jeppesen, P., Mahadevhaiah, S., Burgoyne, P., Wu, R., Gilbert, D. M., Bongiorno, S., Prantera, G., Fanti, L., Pimpinelli, S., Shi, W., Fundele, R., & Singh, P. B. (2004). Heterochromatin and tri-methylated lysine 20 of histone H4 in animals. *Journal of Cell Science*, 117(12), 2491–2501. <https://doi.org/10.1242/jcs.01238>
- Kurz, E. U., & Lees-Miller, S. P. (2004). DNA damage-induced activation of ATM and ATM-dependent signaling pathways. *DNA Repair*, 3(8–9), 889–900. <https://doi.org/10.1016/j.dnarep.2004.03.029>
- Lachner, M., O’Carroll, D., Rea, S., Mechtler, K., & Jenuwein, T. (2001). Methylation of histone H3 lysine 9 creates a binding site for HP1 proteins. *Nature*, 410(6824), 116–120. <https://doi.org/10.1038/35065132>
- Lechner, M. S., Begg, G. E., Speicher, D. W., & Rauscher, F. J. (2000). Molecular Determinants for Targeting Heterochromatin Protein 1-Mediated Gene Silencing: Direct Chromoshadow Domain–KAP-1 Corepressor Interaction Is Essential. *Molecular and Cellular Biology*, 20(17), 6449–6465. <https://doi.org/10.1128/MCB.20.17.6449-6465.2000>

- Lees-Miller, S. P., & Anderson, C. (1989). *The Human Double-stranded DNA-activated Protein Kinase Phosphorylates the 90-kDa Heat-shock Protein, hsp90a at Two NH₂-terminal Threonine Residues*. 6.
- Maher, B. A., Ahmed, I. A. M., Karloukovski, V., MacLaren, D. A., Foulds, P. G., Allsop, D., Mann, D. M. A., Torres-Jardón, R., & Calderon-Garciduenas, L. (2016). Magnetite pollution nanoparticles in the human brain. *Proceedings of the National Academy of Sciences*, 113(39), 10797–10801. <https://doi.org/10.1073/pnas.1605941113>
- Maly, F. E. (1990). The B lymphocyte: A newly recognized source of reactive oxygen species with immunoregulatory potential. *Free Radical Research Communications*, 8(3), 143–148. <https://doi.org/10.3109/10715769009087987>
- Meehan, R. R. (2003). DNA methylation in animal development. *Seminars in Cell & Developmental Biology*, 14(1), 53–65. [https://doi.org/10.1016/S1084-9521\(02\)00137-4](https://doi.org/10.1016/S1084-9521(02)00137-4)
- Mesárošová, M., Kozics, K., Bábelová, A., Regendová, E., Pastorek, M., Vnuková, D., Buliaková, B., Rázga, F., & Gábelová, A. (2014). The role of reactive oxygen species in the genotoxicity of surface-modified magnetite nanoparticles. *Toxicology Letters*, 226(3), 303–313. <https://doi.org/10.1016/j.toxlet.2014.02.025>
- Müller, B., Axelsson, M. D., & Öhlander, B. (2003). Trace elements in magnetite from Kiruna, northern Sweden, as determined by LA-ICP-MS. *GFF*, 125(1), 1–5. <https://doi.org/10.1080/11035890301251001>
- Murrell, G. A., Francis, M. J., & Bromley, L. (1990). Modulation of fibroblast proliferation by oxygen free radicals. *The Biochemical Journal*, 265(3), 659–665. <https://doi.org/10.1042/bj2650659>

- Nikonov, I. N., Folmanis, Yu. G., Folmanis, G. E., Kovalenko, L. V., Laptev, G. Yu., Egorov, I. A., Fisinin, V. I., & Tananaev, I. G. (2011). Iron nanoparticles as a food additive for poultry. *Doklady Biological Sciences*, *440*(1), 328–331.
<https://doi.org/10.1134/S0012496611050188>
- Nissenkorn, A., Levy-Shraga, Y., Banet-Levi, Y., Lahad, A., Sarouk, I., & Modan-Moses, D. (2016). Endocrine abnormalities in ataxia telangiectasia: Findings from a national cohort. *Pediatric Research*, *79*(6), 889–894. <https://doi.org/10.1038/pr.2016.19>
- Noon, A. T., Shibata, A., Rief, N., Löbrich, M., Stewart, G. S., Jeggo, P. A., & Goodarzi, A. A. (2010). 53BP1-dependent robust localized KAP-1 phosphorylation is essential for heterochromatic DNA double-strand break repair. *Nature Cell Biology*, *12*(2), 177–184.
<https://doi.org/10.1038/ncb2017>
- Oberdörster, G. (2000). Pulmonary effects of inhaled ultrafine particles. *International Archives of Occupational and Environmental Health*, *74*(1), 1–8.
<https://doi.org/10.1007/s004200000185>
- O'Neill, T., Dwyer, A. J., Ziv, Y., Chan, D. W., Lees-Miller, S. P., Abraham, R. H., Lai, J. H., Hill, D., Shiloh, Y., Cantley, L. C., & Rathbun, G. A. (2000). Utilization of Oriented Peptide Libraries to Identify Substrate Motifs Selected by ATM. *Journal of Biological Chemistry*, *275*(30), 22719–22727. <https://doi.org/10.1074/jbc.M001002200>
- Peters, A. H. F. M., O'Carroll, D., Scherthan, H., Mechtler, K., Sauer, S., Schöfer, C., Weipoltshammer, K., Pagani, M., Lachner, M., Kohlmaier, A., Opravil, S., Doyle, M., Sibilia, M., & Jenuwein, T. (2001). Loss of the Suv39h Histone Methyltransferases Impairs Mammalian Heterochromatin and Genome Stability. *Cell*, *107*(3), 323–337.
[https://doi.org/10.1016/S0092-8674\(01\)00542-6](https://doi.org/10.1016/S0092-8674(01)00542-6)

- Petrini, J. H. (2000). The Mre11 complex and ATM: Collaborating to navigate S phase. *Current Opinion in Cell Biology*, 12(3), 293–296. [https://doi.org/10.1016/S0955-0674\(00\)00091-0](https://doi.org/10.1016/S0955-0674(00)00091-0)
- Pilch, D. R., Sedelnikova, O. A., Redon, C., Celeste, A., Nussenzweig, A., & Bonner, W. M. (2003). Characteristics of γ -H2AX foci at DNA double-strand breaks sites. *Biochemistry and Cell Biology*, 81(3), 123–129. <https://doi.org/10.1139/o03-042>
- Plath, K., Fang, J., Mlynarczyk-Evans, S. K., Cao, R., Worringer, K. A., Wang, H., Cruz, C. C. de la, Otte, A. P., Panning, B., & Zhang, Y. (2003). Role of Histone H3 Lysine 27 Methylation in X Inactivation. *Science*, 300(5616), 131–135. <https://doi.org/10.1126/science.1084274>
- Riballo, E., Doherty, A., Smith, G. C. M., Recio, M.-J., Reis, C., Dahm, K., Fricke, A., Krempler, A., Parker, A. R., Jackson, S. P., Gennery, A., & Jeggo, P. A. (2004). A Pathway of Double-Strand Break Rejoining Dependent upon ATM, Artemis, and Proteins Locating to γ -H2AX Foci. *Molecular Cell*, 10.
- Riboldi, G. M., Samanta, D., & Frucht, S. (2020). Ataxia Telangiectasia (Louis-Bar Syndrome). In *StatPearls*. StatPearls Publishing. <http://www.ncbi.nlm.nih.gov/books/NBK519542/>
- Rogakou, E. P., Boon, C., Redon, C., & Bonner, W. M. (1999). Megabase Chromatin Domains Involved in DNA Double-Strand Breaks in Vivo. *Journal of Cell Biology*, 146(5), 905–916. <https://doi.org/10.1083/jcb.146.5.905>
- Rothblum-Oviatt, C., Wright, J., Lefton-Greif, M. A., McGrath-Morrow, S. A., Crawford, T. O., & Lederman, H. M. (2016). Ataxia telangiectasia: A review. *Orphanet Journal of Rare Diseases*, 11(1), 159. <https://doi.org/10.1186/s13023-016-0543-7>

- Saito, S., Goodarzi, A. A., Higashimoto, Y., Noda, Y., Lees-Miller, S. P., Appella, E., & Anderson, C. W. (2002). ATM Mediates Phosphorylation at Multiple p53 Sites, Including Ser⁴⁶, in Response to Ionizing Radiation. *Journal of Biological Chemistry*, 277(15), 12491–12494. <https://doi.org/10.1074/jbc.C200093200>
- Schultz, D. C., Ayyanathan, K., Negorev, D., Maul, G. G., & Rauscher, F. J. (2002). SETDB1: A novel KAP-1-associated histone H3, lysine 9-specific methyltransferase that contributes to HP1-mediated silencing of euchromatic genes by KRAB zinc-finger proteins. *Genes & Development*, 16(8), 919–932. <https://doi.org/10.1101/gad.973302>
- Schultz, D. C., Friedman, J. R., & Rauscher, F. J. (2001). Targeting histone deacetylase complexes via KRAB-zinc finger proteins: The PHD and bromodomains of KAP-1 form a cooperative unit that recruits a novel isoform of the Mi-2 α subunit of NuRD. *Genes & Development*, 15(4), 428–443. <https://doi.org/10.1101/gad.869501>
- Sheykhbaglou, R., Sedghi, M., Shishevan, M. T., & Sharifi, R. S. (2010). Effects of Nano-Iron Oxide Particles on Agronomic Traits of Soybean. *Notulae Scientia Biologicae*, 2(2), 112–113. <https://doi.org/10.15835/nsb224667>
- Shiloh, Y. (1997). ATAXIA-TELANGIECTASIA AND THE NIJMEGEN BREAKAGE SYNDROME: Related Disorders But Genes Apart. *Annual Review of Genetics*, 31(1), 635–662. <https://doi.org/10.1146/annurev.genet.31.1.635>
- Shiloh, Yosef. (2003). ATM and related protein kinases: Safeguarding genome integrity. *Nature Reviews Cancer*, 3(3), 155–168. <https://doi.org/10.1038/nrc1011>
- Siliciano, J. D., Canman, C. E., Taya, Y., Sakaguchi, K., Appella, E., & Kastan, M. B. (1997). DNA damage induces phosphorylation of the amino terminus of p53. *Genes & Development*, 11(24), 3471–3481. <https://doi.org/10.1101/gad.11.24.3471>

- Sims, R. J., Nishioka, K., & Reinberg, D. (2003). Histone lysine methylation: A signature for chromatin function. *Trends in Genetics*, *19*(11), 629–639.
<https://doi.org/10.1016/j.tig.2003.09.007>
- Sonmez, E., Aydin, E., Turkez, H., Özbek, E., Togar, B., Meral, K., Çetin, D., Cacciatore, I., & di, S. (2016). Cytotoxicity and genotoxicity of iron oxide nanoparticles: An in vitro biosafety study. *Archives of Biological Sciences*, *68*(1), 41–50.
<https://doi.org/10.2298/ABS141218006S>
- Sowards, J. W., Lippold, J. C., Dickinson, D. W., & Ramirez, A. J. (2008). *Characterization of Welding Fume from SMAW Electrodes—Part I. 7.*
- Tran, C. L., Cullen, R. T., Buchanan, D., Searl, A., & Jones, A. D. (2000). INHALATION OF POORLY SOLUBLE PARTICLES. II. INFLUENCE OF PARTICLE SURFACE AREA ON INFLAMMATION AND CLEARANCE. *Inhalation Toxicology*, *12*(12), 1113–1126.
<https://doi.org/10.1080/08958370050166796>
- Urnov, F. D. (2002). A feel for the template: Zinc finger protein transcription factors and chromatin. *Biochemistry and Cell Biology*, *80*(3), 321–333. <https://doi.org/10.1139/o02-084>
- Valdiglesias, V., Kiliç, G., Costa, C., Fernández-Bertólez, N., Pásaro, E., Teixeira, J. P., & Laffon, B. (2015). Effects of iron oxide nanoparticles: Cytotoxicity, genotoxicity, developmental toxicity, and neurotoxicity: Effects of Iron Oxide Nanoparticles. *Environmental and Molecular Mutagenesis*, *56*(2), 125–148.
<https://doi.org/10.1002/em.21909>
- Valko, M., Morris, H., & Cronin, M. (2005). Metals, Toxicity and Oxidative Stress. *Current Medicinal Chemistry*, *12*(10), 1161–1208. <https://doi.org/10.2174/0929867053764635>

- van der Vlag, J., & Otte, A. P. (1999). Transcriptional repression mediated by the human polycomb-group protein EED involves histone deacetylation. *Nature Genetics*, *23*(4), 474–478. <https://doi.org/10.1038/70602>
- Voinov, M. A., Pagán, J. O. S., Morrison, E., Smirnova, T. I., & Smirnov, A. I. (2011). Surface-Mediated Production of Hydroxyl Radicals as a Mechanism of Iron Oxide Nanoparticle Biototoxicity. *Journal of the American Chemical Society*, *133*(1), 35–41. <https://doi.org/10.1021/ja104683w>
- Wade, P. A. (2001). Methyl CpG-binding proteins and transcriptional repression*. *BioEssays*, *23*(12), 1131–1137. <https://doi.org/10.1002/bies.10008>
- White, D., Rafalska-Metcalf, I. U., Ivanov, A. V., Corsinotti, A., Peng, H., Lee, S.-C., Trono, D., Janicki, S. M., & Rauscher, F. J. (2012). The ATM Substrate KAP1 Controls DNA Repair in Heterochromatin: Regulation by HP1 Proteins and Serine 473/824 Phosphorylation. *Molecular Cancer Research*, *10*(3), 401–414. <https://doi.org/10.1158/1541-7786.MCR-11-0134>
- Wu, H., Yin, J.-J., Wamer, W. G., Zeng, M., & Lo, Y. M. (2014). Reactive oxygen species-related activities of nano-iron metal and nano-iron oxides. *Journal of Food and Drug Analysis*, *22*(1), 86–94. <https://doi.org/10.1016/j.jfda.2014.01.007>
- Zaki-Dizaji, M., Akrami, S. M., Abolhassani, H., Rezaei, N., & Aghamohammadi, A. (2017). Ataxia telangiectasia syndrome: Moonlighting ATM. *Expert Review of Clinical Immunology*, *13*(12), 1155–1172. <https://doi.org/10.1080/1744666X.2017.1392856>
- Zhang, W. (2003). *Nanoscale Iron Particles for Environmental Remediation: An Overview*. 10.
- Ziv, Y., Bielopolski, D., Galanty, Y., Lukas, C., Taya, Y., Schultz, D. C., Lukas, J., Bekker-Jensen, S., Bartek, J., & Shiloh, Y. (2006). Chromatin relaxation in response to DNA

double-strand breaks is modulated by a novel ATM- and KAP-1 dependent pathway.

Nature Cell Biology, 8(8), 870–876. <https://doi.org/10.1038/ncb1446>

Table of chemical reactions:

$\text{Fe}^{2+} + \text{H}_2\text{O}_2 \longrightarrow \text{Fe}^{3+} + \text{OH}^- + \text{OH}^\bullet$	1	18
$\text{Fe}^{3+} + \text{O}_2^- \longrightarrow \text{Fe}^{2+} + \text{O}_2$	2	18
$2\text{O}_2^- + 2\text{H}^+ \longrightarrow \text{H}_2\text{O}_2 + \text{O}_2$	3	18
$\text{Fe}^{2+} + \text{O}_2 \longrightarrow \text{Fe}^{4+} \text{O}^{2-}$	4	18
$\text{Fe}^{2+} + \text{O}_2 \longrightarrow \text{Fe}^{3+} + \text{HO}_2^\bullet/\text{O}_2^{\bullet-}$	5	19
$\text{OH}^\bullet + \text{H}_2\text{O}_2 \longrightarrow \text{H}_2\text{O} + \text{H}^+ + \text{O}_2^-$	6	19
$\text{OH}^\bullet + \text{Fe}^{2+} \longrightarrow \text{Fe}^{3+} + \text{OH}^-$	7	19
$\text{LOOH} + \text{Fe}^{2+} \longrightarrow \text{Fe}^{3+} + \text{LO}^- + \text{OH}^\bullet$	8	19